AD 729448

AFCRL-71-0233
23 APRIL 1971
ENVIRONMENTAL RESEARCH PAPERS, NO. 351

AIR FORCE CAMBRIDGE RESEARCH LABORATORIES
L. G. HANSCOM FIELD, BEDFORD, MASSACHUSETTS

Application of Vector and Matrix Methods to Triangulation of Chemical Releases in the Upper Atmosphere

ANTONIO F. QUESADA

DDC
RECEIVED
SEP 13 1971
A

This document has been approved for public release and sale; its distribution is unlimited

Reproduced by
NATIONAL TECHNICAL
INFORMATION SERVICE
Springfield, Va. 22151

AIR FORCE SYSTEMS COMMAND
United States Air Force

61

Unclassified

Security Classification

DOCUMENT CONTROL DATA - R&D

(Security classification of title, body of abstract and indexing annotation must be entered when the overall report is classified)

1. ORIGINATING ACTIVITY *(Corporate author)* Air Force Cambridge Research Laboratories (LKC) L. G. Hanscom Field Bedford, Massachusetts 01730	2a. REPORT SECURITY CLASSIFICATION Unclassified 2b. GROUP

3. REPORT TITLE

APPLICATION OF VECTOR AND MATRIX METHODS TO TRIANGULATION OF CHEMICAL RELEASES IN THE UPPER ATMOSPHERE

4. DESCRIPTIVE NOTES *(Type of report and inclusive dates)*

Scientific. Interim.

5. AUTHOR(S) *(First name, middle initial, last name)*

Antonio F. Quesada

6. REPORT DATE 23 April 1971	7a. TOTAL NO. OF PAGES 59	7b. NO. OF REFS 12

8a. CONTRACT OR GRANT NO.	9a. ORIGINATOR'S REPORT NUMBER(S) AFCRL-71-0233
b. PROJECT, TASK, WORK UNIT NOS. 7635-13-01 c. DOD ELEMENT 62101F d. DOD SUBELEMENT 681000	9b. OTHER REPORT NO(S) *(Any other numbers that may be assigned this report)* ERP No. 351

10. DISTRIBUTION STATEMENT

1-This document has been approved for public release and sale; its distribution is unlimited.

11. SUPPLEMENTARY NOTES TECH, OTHER	12. SPONSORING MILITARY ACTIVITY Air Force Cambridge Research Laboratories (LKC) L. G. Hanscom Field Bedford, Massachusetts 01730

13. ABSTRACT

The methodology of vector and matrix algebra has been used to simplify the triangulation procedures required to determine the position, motion, and growth of luminescent gas clouds injected into the upper atmosphere. Generated by chemicals discharged from rockets programed to effect point or continuous releases at preselected times, such clouds have proved to be a powerful experimental tool for gathering data relevant to upper atmosphere phenomena such as winds, wind shears, and turbulent transport mechanisms, and the production, maintenance, and decay of ionization in support of specific Air Force requirements in satellite operations, missile detection, and communications.

Details of illustrations in this document may be better studied on microfiche

DD FORM 1 NOV 65 1473

Unclassified

Security Classification

Unclassified

Security Classification

14. KEY WORDS	LINK A ROLE	LINK A WT	LINK B ROLE	LINK B WT	LINK C ROLE	LINK C WT
Chemical releases						
Triangulation						
Position measurements in the upper atmosphere						
Photographic triangulation						
Coordinate transformations						

Unclassified

Security Classification

AFCRL-71-0233
23 APRIL 1971
ENVIRONMENTAL RESEARCH PAPERS, NO. 351

AERONOMY LABORATORY PROJECT 7635

AIR FORCE CAMBRIDGE RESEARCH LABORATORIES
L. G. HANSCOM FIELD, BEDFORD, MASSACHUSETTS

Application of Vector and Matrix Methods to Triangulation of Chemical Releases in the Upper Atmosphere

ANTONIO F. QUESADA

Details of illustrations in
this document may be better
studied on microfiche

This document has been approved for public release and sale; its distribution is unlimited

AIR FORCE SYSTEMS COMMAND
United States Air Force

Abstract

The methodology of vector and matrix algebra has been used to simplify the triangulation procedures required to determine the position, motion, and growth of luminescent gas clouds injected into the upper atmosphere. Generated by chemicals discharged from rockets programed to effect point or continuous releases at preselected times, such clouds have proved to be a powerful experimental tool for gathering data relevant to upper atmosphere phenomena such as winds, wind shears, and turbulent transport mechanisms, and the production, maintenance, and decay of ionization in support of specific Air Force requirements in satellite operations, missile detection, and communications.

Contents

1. INTRODUCTION 1

2. THE COORDINATE SYSTEMS 3

3. COORDINATE TRANSFORMATIONS 8

4. ORIENTATION OF THE CAMERA SYSTEM 18

5. TRIANGULATION PROCEDURE FOR POINT RELEASES 23

6. TRIANGULATION ON CONTINUOUS TRAILS 28

7. TRANSFORMATIONS TO OTHER REFERENCE SYSTEMS 34

7.1 Geodetic Coordinates 34
7.2 Geodetic to Geocentric Coordinates 36
7.3 Geocentric to Geodetic Coordinates 37
7.4 Geocentric to Horizon Coordinates 38
7.5 Horizon to Geocentric Coordinates (special case) 40
7.6 Camera to Horizon Coordinates 40
7.7 Horizon to Camera Coordinates 41

REFERENCES 45

APPENDIX A: Parametric Cubic Splines 47

APPENDIX B: Lagrange's Expansion 53

APPENDIX C: Useful Constants 55

Illustrations

1.	Equatorial Coordinate System	4
2.	Geocentric Coordinate System	6
3.	Camera Coordinate System	7
4.	Relation Between Geocentric and Equatorial Systems	10
5.	Relation Between Camera and Equatorial Systems	11
6.	Relation Between Camera and Geocentric Systems	14
7.	Coordinate Systems on the Film Plane	15
8.	Triangulation on Point Releases	25
9.	Luminescent Trail as Observed From Two Different Triangulation Sites	29
10.	Triangulation on Trails	30
11.	Geodetic System of Coordinates	35
A1.	Example of Curve-fitting by Means of Parametric Cubic Splines	51

Application of Vector and Matrix Methods to Triangulation of Chemical Releases in the Upper Atmosphere

I. INTRODUCTION

Photographic data taken from ground stations for the purpose of determining the position, motion, and growth of luminescent clouds and trails have for a number of years been reduced and analyzed by various procedures (Refs. 2, 5, 6, 7, 8, 12). The artificial clouds and trails are generated by discharging chemicals into the upper atmosphere from rockets programed to effect point or continuous releases at preselected times. They have proved to be a powerful experimental tool for the study of various upper atmosphere phenomena, including winds, wind shears, and turbulent transport mechanisms.

The triangulation techniques applied to the data differ according to the type of release whose evolution is recorded on the film being processed. As might be anticipated, the analysis becomes simpler for discrete puffs possessing structural features that can be clearly identified from two or more ground stations. A more complex mathematical problem is presented by diffuse clouds and continuous trails with few or no distinctive features that can be unambiguously matched on the film records corresponding to views of the release from different triangulation sites.

The present report describes an attempt to simplify reduction and interpretation of the photographic data and increase accuracy and reliability of the results by (a) devising analytic procedures that consistently discard superfluous coordinate

(Received for publication 23 April 1971)

transformations, (b) try to develop formulas that are symmetric with respect to the observation sites, (c) establish direct analytic criteria for determining coordinates of the cloud features under observation, and (d) use redundancy to check the consistency of previously determined results. The reduction in the number of coordinate transformations leads to a conceptually simpler computational scheme, and as direct consequence of fewer arithmetical operations having to be performed on the original data, the accuracy of the results is degraded to a lesser degree.

Mathematical formulation of the triangulation problem becomes very straightforward by systematic use of vector algebra and analysis. Recognition of the vector character of the positional data allows many of the expressions to be written in invariant fashion, and the coordinate transformations become simple rotations and translations. The abstract properties of the corresponding operators are realized by well-known matrices, and the entire scheme can be cast into a form that can be generalized with minimum effort. The resultant expressions are extremely compact and can often be readily grouped into symmetric combinations in which data from all sites play equal roles. Aside from the fact that there is generally no a priori reason for assigning a preferential position to a given site, an advantage of such a scheme is that special or singular cases and the concomitant lengthening and increased complexity of the computer codes needed to implement the mathematical formalism are avoided. As a further advantage, well-known vector identities can be used to check the consistency of the results.

It is hoped that the organization of the material will allow the reader to follow development of the thesis without undue effort. At the outset we recognize that the triangulation problem can be divided into independent units. Some are repeatedly used during analysis of a batch of data. Others are needed only to fix the orientation of the cameras and are not recalled unless the cameras are moved during the time it takes to photograph the entire sequence of events associated with the deposition, growth, and decay of a chemical release. Orientation and some optical parameters of the camera can be accurately determined by photographing the stellar background shortly before the rocket and its chemical payload are launched. Stars can be readily identified and their positions on the photographic plate can be measured very precisely. The plane of the photographic plate and the line of sight along the camera optic axis serve to define one of the coordinate systems of direct interest to us.* The other systems are the equatorial system, traditionally used

*In the discussion presented here it is assumed that a perfect camera is used. Performance of actual cameras must be corrected for such defects as shift of center of frame from trace of optic axis, departure of film plane from perpendicularity to optic axis, lens distortion, and film shrinkage. The analysis remains unaltered if it is understood that appropriate corrections have been applied to all film measurements. For procedures to evaluate the corrections, see Justus (1963).

by astronomers as a frame of reference for star locations, and a cartesian geocentric system with its origin at the center of the earth, its +z axis along the line joining the origin and the North Pole, its +x axis coincident with the line joining the origin and the point on the equator intersected by the prime meridian (Greenwich), and its +y axis completing a righthanded orthogonal triad. In view of the fact that our observations are made from stations riding on the earth, it is advantageous to think of this geocentric system as a preferred frame of reference and to regard geocentric coordinates as canonical coordinates for all events. In particular, this will simplify the conversion from equatorial coordinates as well as the conversion to two auxiliary systems we shall use on occasion: an azimuth-elevation—slant range system and the geodetic system of longitude, latitude, and altitude above surface of a reference ellipsoid.

Section 2 deals with the basic coordinate systems. The coordinate transformations are developed in Sec. 3; in Sec. 4 they are applied to the previously defined systems. At this point we have sufficient information to deal with the problem of determining the geocentric coordinates of a point release observed from two or more stations. This constitutes the bulk of Sec. 5.

Section 6 describes the more elaborate procedure that is needed to triangulate on thin, continuous trails of lengths measured in tens of kilometers. The most vexing problem associated with these trails is the difficulty of matching corresponding points on photographs taken at different times or from different stations. The procedure we follow is to select a point on one view and search for its image on a second view after the trail has been replaced by a two-dimensional curve on the plate plane, which is itself represented analytically by a parametric cubic spline. The introduction of parametric representations is mandatory, to deal with multivaluedness created by selfintersections or pronounced twisting of the trail and its replacement curve. Since very little can be found in the literature on parametric splines, the general procedure needed to determine the sets of polynomial coefficients is described in Appendix A.

Section 7 deals with coordinate transformations between geodetic and geocentric, geocentric and horizon, and camera and horizon, systems.

Since all geodetic reference ellipsoids have very small eccentricities, it was found convenient to make use of the Lagrange expansion. A statement of the expansion in its full generality is given separately in Appendix B. Appendix C lists a short table of useful constants.

2. THE COORDINATE SYSTEMS

Systems of reference for astronomical purposes are constructed by selecting a great circle on the celestial sphere and one point on that circle. Spherical

coordinates are then introduced to specify the position of points on the sphere: one coordinate measured perpendicular to the selected great circle along an auxiliary great circle; the second measured from the selected point to the point of intersection of the auxiliary circle.

The fundamental astronomical reference systems are based on the celestial equator and the ecliptic. Angular coordinates in these planes are measured from the ascending node of the ecliptic on the celestial equator, customarily referred to as the vernal equinox, the first point of Aries, or simply the equinox, and denoted by ♈. Only the first of these systems is relevant to our discussion.

A righthanded cartesian coordinate system with its origin at the center of the earth can be constructed by directing the +x axis toward the equinox, the +y axis to a point $\pi/2$ radians to the east in the plane of the celestial equator, the +z axis pointing north to the pole. This is the equatorial system, shown schematically in Figure 1. To specify the location of very distant points it is sufficient to give the angular coordinates that identify a direction—customarily the angles α and δ, which denote the right ascension and declination, respectively. Clearly, α and $(\pi/2)-\delta$ are the familiar spherical coordinates corresponding to that direction in

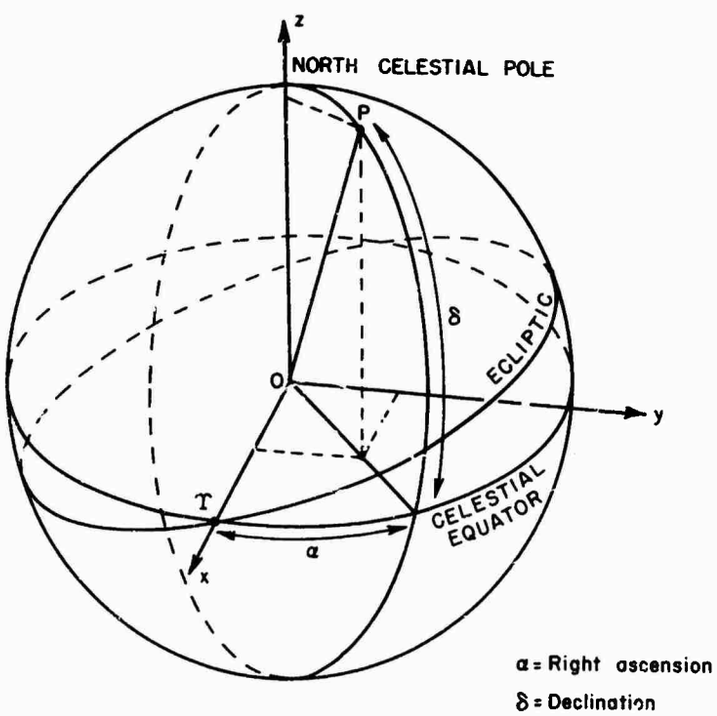

Figure 1. Equatorial Coordinate System

space. If necessary, the same direction can be identified by the unit vector $\hat{e}$, having the cartesian representation

$$\hat{e} = \hat{x}\,(\cos\alpha\,\cos\delta) + \hat{y}\,(\sin\alpha\,\cos\delta) + \hat{z}\,\sin\delta\,. \tag{1}$$

Any point along the line OP can then be represented by the vector

$$\vec{r} = r\,\hat{e}, \tag{2}$$

where r denotes the distance from O.

The declination is measured in degrees, minutes, and seconds along the great circle through the observed body and the pole. Right ascension is measured in hours, minutes, and seconds from ♈ along the equator in the west-east direction, that is, opposite to the apparent rotation of the celestial sphere. The conversion to the equivalent angular measure offers no difficulty.

Since observations are made from the surface of the earth, topocentric coordinate systems with origin at the observer are of importance. The reduction from earth-centered to topocentric coordinates depends in part on the figure of the earth and will be considered in later sections.

For our purposes it is advantageous to introduce as the primary geocentric system a righthanded cartesian system fixed in the earth, with the +z axis pointing north, and the equator lying in the xy plane. The +x axis is directed toward the intercept of the equator and a prime meridian (Greenwich, for example). The +y axis completes an orthogonal triad (see Figure 2). The context will be sufficient to distinguish this system from others that share the same origin. The angular coordinates of this geocentric system will be described by using λ and ϕ' to denote the longitude and geocentric latitude, respectively. A unit vector $\hat{g}$, which in the geocentric system can be written in component form as

$$\hat{g} = \hat{x}\,(\cos\lambda\,\cos\phi') + \hat{y}\,(\sin\lambda\,\cos\phi') + \hat{z}\,\sin\phi'\,, \tag{3}$$

corresponds to the direction specified by the coordinates (λ, ϕ'). The position vector

$$\vec{r} = r\hat{g} \tag{4}$$

corresponds to a point along this direction, r units away from the origin.

The basic topocentric system of interest to us is determined by the cameras that record the evolution of the chemical releases.

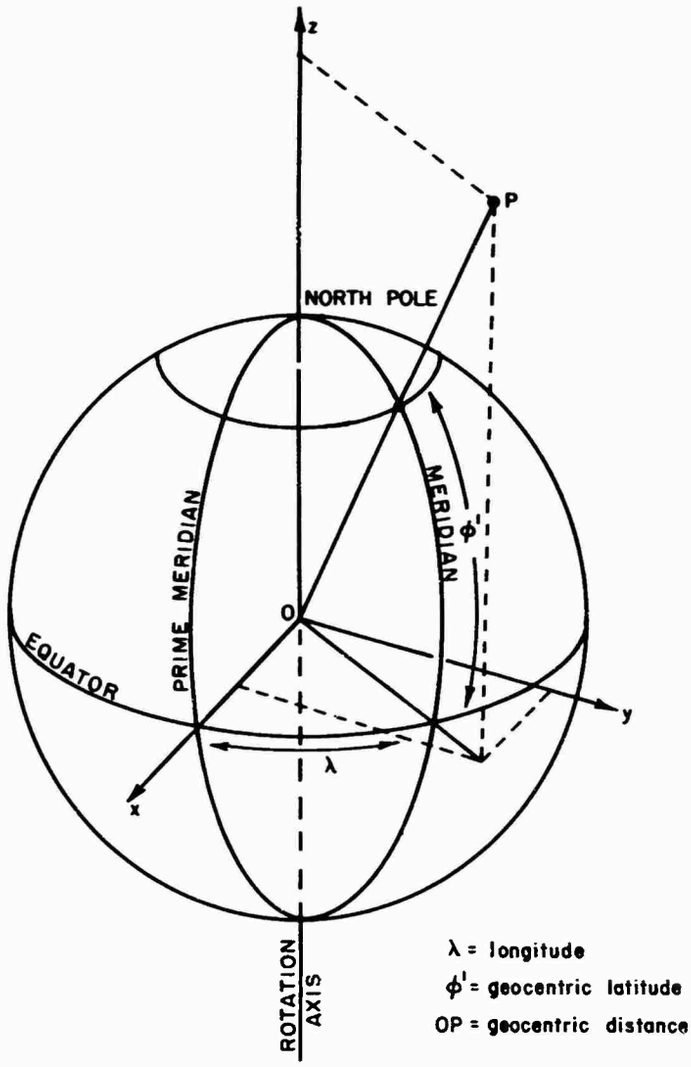

Figure 2. Geocentric Coordinate System

The +z axis of the coordinate system associated with the camera at a given observation site points in the direction of the optic axis of the camera lenses. The xy plane is perpendicular to this axis and passes through the image nodal point of the optical system. The selection of x and y directions in this plane is arbitrary. It is convenient to take the x axis parallel to one of the edges of the picture frame, or along the direction determined by appropriate fiducial marks that appear on each exposure. The y axis is chosen to complete a righthanded orthogonal system.

As indicated in the footnote in the introduction, it will be assumed that an ideal camera system is used at each observation site. This means, for instance, that the film plane is strictly parallel to the xy coordinate plane and is normal to the optic axis. It also presupposes that the optical system is totally free of distortion, field curvature, and chromatic aberration. When these conditions are satisfied, distance measurements on the image plane can be readily converted into angular measurements relative to the topocentric coordinate system defined above. From Figure 3 it follows that:

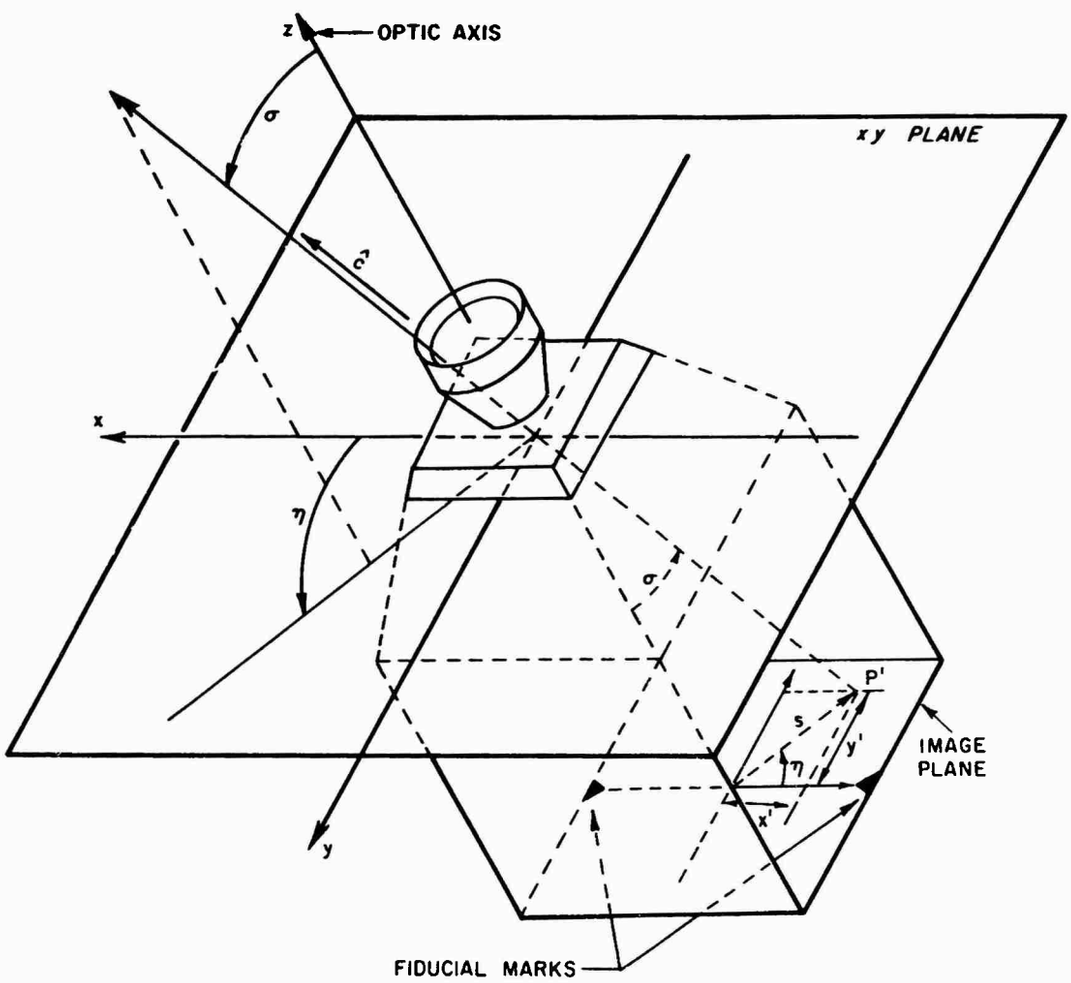

Figure 3. Camera Coordinate System

$$\tan\sigma = \frac{s}{f} = \sqrt{\frac{(x')^2 + (y')^2}{f}}\,, \tag{5}$$

$$\sin\eta = \frac{y'}{s}\,, \tag{6}$$

$$\cos\eta = \frac{x'}{s}\,. \tag{7}$$

The unit vector $\hat{c}$, along the line of sight to a point whose image is found at P', is therefore

$$\hat{c} = \hat{x}\,(\sin\sigma\cos\eta) + \hat{y}\,(\sin\sigma\sin\eta) + \hat{z}\cos\sigma\ . \tag{8}$$

The coordinates σ and η specify a direction in space with respect to a camera system defined by a camera whose effective focal length is f. A space point r units distant from the origin, in the direction of the vector $\hat{c}$, is represented by the position vector

$$\vec{r} = r\hat{c}\ . \tag{9}$$

This completes our discussion of the basic coordinate systems needed to describe the positions of points on the clouds and trails used for the study of upper atmosphere phenomena. The auxiliary systems mentioned earlier will be introduced in Sec. 7. We will now relate these systems in order to refer all observations to a single system before we perform the data manipulation that will enable us to extract physically significant information from the raw photographic data.

3. COORDINATE TRANSFORMATIONS

The position of a point in space is specified by coordinates referred to a system that is to a great extent selected arbitrarily but is often governed by tradition or preferred for reasons of convenience or simplicity. Since photographic data to evaluate the motion and growth of chemical releases in the upper atmosphere are taken from stations that move with the earth, it has been found simpler and more convenient to refer the coordinates of points on clouds and trails to the geocentric system defined in Sec. 2. To accomplish this it is necessary to relate the geocentric and the camera systems, that is, we must know the geocentric orientation of the cameras. An accurate and reliable way of determining this orientation consists in photographing the stellar background shortly before a chemical release takes place. In view of the fact that the star coordinates

generally listed in star catalogs are right ascension and declination, it also becomes necessary to find the transformation from equatorial to geocentric coordinates. This transformation is a simple two-dimensional rotation because the two systems have a common origin and coincident z axes. The transformation from camera to equatorial or geocentric coordinates is more involved and in its general form can be decomposed into a three-dimensional rotation followed by a translation.

A simplification occurs in photography of the stellar background. The very great distances involved validate the assumption that stars are essentially at infinity, and the error introduced by a parallel translation of the camera system from the earth's surface until its origin coincides with the center of the earth is therefore negligible. The transformation between the camera and equatorial or geocentric coordinates consequently becomes a general rotation of axes.

It is well known that rotations can be regarded as transformations effected by operators that can be represented by 3×3 orthogonal matrices. The general matrix can be generated by multiplication, in an appropriate order, of matrices representing simple rotations about a coordinate axis. These rotation matrices, denoted by $R_i(\theta)$—the subscript refers to the axis of rotation, with i = 1, 2, 3 denoting the x, y, z axes, respectively—have elements a_{ij} that satisfy the conditions (Kaula, 1966):

$$j - 1 \equiv i \pmod 3 ;$$

$$k - 2 \equiv i \pmod 3 ;$$

$$a_{ii} = 1, \quad a_{jj} = a_{kk} = \cos\theta ;$$

$$a_{ij} = a_{ji} = a_{ik} = a_{ki} = 0, \quad a_{jk} = -a_{kj} = \sin\theta . \tag{10}$$

The signs apply to righthanded systems, for counterclockwise rotations as viewed from a point on the positive half of the axis looking toward the origin. For example, for rotations about the z axis, we have

$$R_z(\theta) = \begin{pmatrix} \cos\theta & \sin\theta & 0 \\ -\sin\theta & \cos\theta & 0 \\ 0 & 0 & 1 \end{pmatrix}. \tag{11}$$

In the particular case of conversion from equatorial to geocentric coordinates we have angle θ = GHA T. The connections between the various angles are shown in Figure 4, which depicts the apparent motion of the equatorial frame as viewed

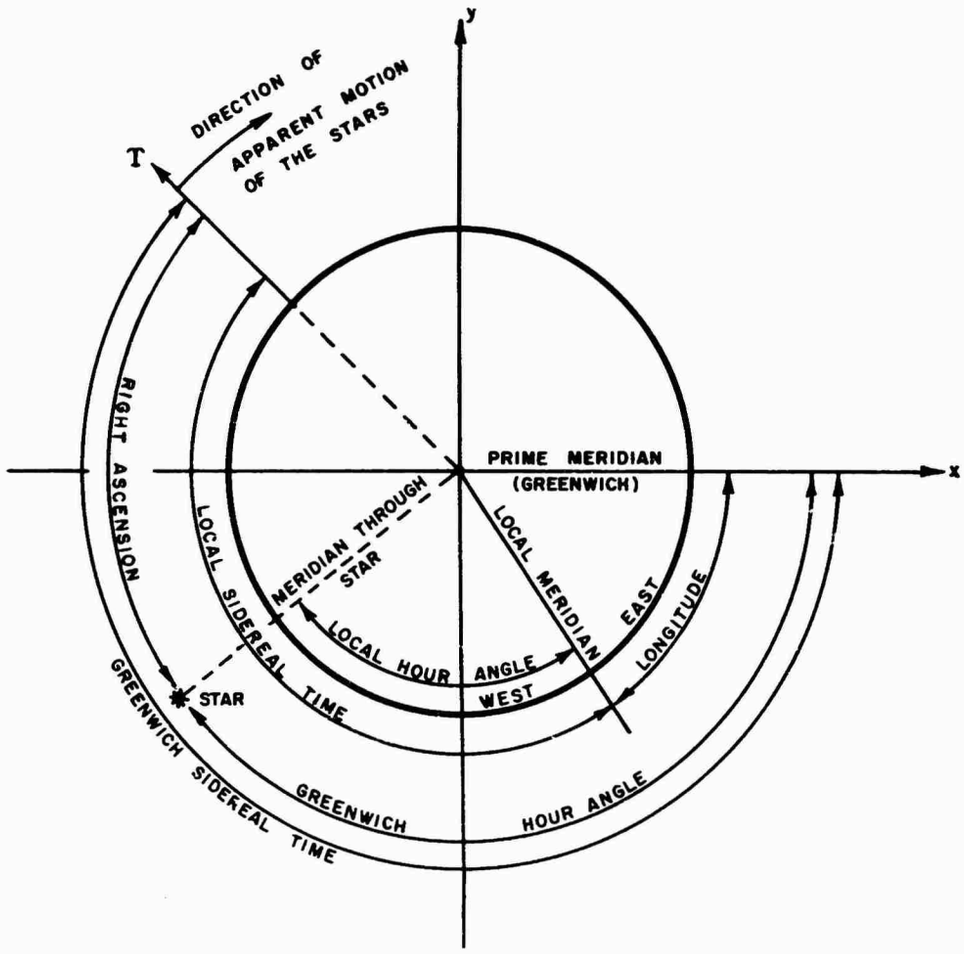

Figure 4. Relation Between Geocentric and Equatorial Systems

by an observer in the geocentric system. It is conventional to measure hour angles positive westward, from the local meridian to the hour circle of the star. The hour angle of the equinox is, by definition, the sidereal time. Let h and h_G be the local and Greenwich hour angles of a star whose right ascension is α. Similarly, let τ and τ_G be the corresponding sidereal times. Then, from Figure 4, we have that at the instant a star is observed,

$$\tau = \mathrm{LST} = h + \alpha \,, \tag{12}$$

$$\tau_G = \mathrm{GST} = h_G + \alpha = \tau + \lambda \,, \tag{13}$$

and

$$h_G = \tau + \lambda - \alpha \,. \tag{14}$$

It is clear from the diagram that we must set $\theta = \tau_G$.

The transformation connecting the camera and the equatorial systems will now be discussed. As indicated earlier, for the stellar background we can use a pure rotation. Figure 5 shows (a) the basic geometry in these circumstances, and (b) how the general rotation can be decomposed into three simple rotations: (1) about the z axis (earth's polar axis), (2) about the y' axis, and (3) about the z" axis. The rotation angles are therefore the well-known Euler angles.

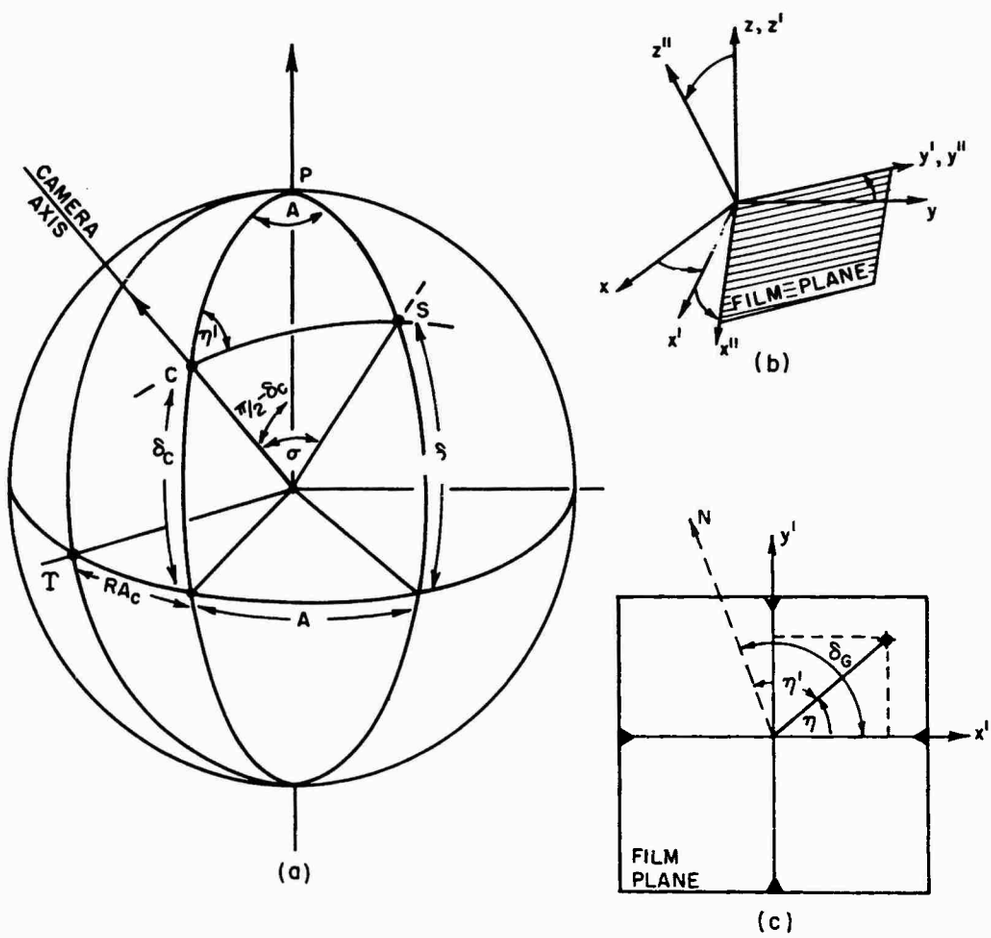

Figure 5. Relation Between Camera and Equatorial Systems

Let α_c and δ_c be the right ascension and declination, respectively, of the point on the celestial sphere that marks the direction in space along the camera optic axis. Let σ, η', and A be one side and two angles of the spherical triangle formed by the camera axis intercept C, the star S, and the pole P. On the photographic plate the star image appears as in Figure 5(c). If the star coordinates (right ascension and declination) are α and δ, respectively, we have:

$$\begin{pmatrix} \cos\eta \sin\sigma \\ \sin\eta \sin\sigma \\ \cos\sigma \end{pmatrix} = R_z(\delta\epsilon) R_y\left(\frac{\pi}{2} - \delta_c\right) R_z\left(\alpha_c\right) \begin{pmatrix} \cos\alpha \cos\delta \\ \sin\alpha \cos\delta \\ \sin\delta \end{pmatrix}, \tag{15}$$

where $R_z(\delta\epsilon)$ and $R_z(\alpha_c)$ are given by Eq. (11), with $\theta = \delta\epsilon$ and $\theta = \alpha_c$, respectively, and

$$R_y\left(\frac{\pi}{2} - \delta_c\right) = \begin{pmatrix} \sin\delta_c & 0 & -\cos\delta_c \\ 0 & 1 & 0 \\ \cos\delta_c & 0 & \sin\delta_c \end{pmatrix}. \tag{16}$$

The column vectors will be recognized as alternative representations of the unit vector along the direction of the star in the two coordinate systems. The components were displayed in Eqs. (8) and (1). Equation (15) can be simplified for $\delta\epsilon = 0$ or $\delta\epsilon = \pi/2$. In the former case it can be written in expanded form as

$$\cos\delta \cos\alpha \cos\alpha_c \sin\delta_c + \cos\delta \sin\alpha \sin\alpha_c \sin\delta_c - \sin\delta \cos\delta_c = \cos\eta \sin\sigma, \tag{17a}$$

$$-\cos\delta \cos\alpha \sin\alpha_c + \cos\delta \sin\alpha \cos\alpha_c = \sin\eta \sin\sigma, \tag{17b}$$

$$\cos\delta \cos\alpha \cos\alpha_c \cos\delta_c + \cos\delta \sin\alpha \sin\alpha_c \cos\delta_c + \sin\delta \sin\delta_c = \cos\sigma, \tag{17c}$$

which can be solved explicitly for δ and α in terms of η and σ. We can easily verify the results

$$\tan(\alpha - \alpha_c) = \frac{\sin\eta \sin\sigma}{\cos\sigma \cos\delta_c + \sin\sigma + \sin\delta_c \cos\eta} \tag{18a}$$

and

$$\sin\delta = \sin\delta_c \cos\sigma - \cos\delta_c \sin\sigma \cos\eta \,. \tag{18b}$$

These expressions, or the more general ones that can be derived from Eq. (15) with $\delta\epsilon \neq 0$, allow us to compute the right ascension and declination of an object whose image coordinates have been measured and used for evaluating the angles σ and η [Eqs. (5), (6), and (7)]. This is seldom the way Eq. (15) is used, however. The primary reason for establishing Eq. (15) is to have the means of determining the orientation of the camera system from photographs of the stellar background at the observation site. Details of the procedure are given in Sec. 4. Let us, for the moment, assume that α_c and δ_c are known. It follows, then, that in the equatorial system a unit vector $\hat{n}$ in the direction of the camera axis has the form

$$(\hat{n})_E = \hat{x}_E\,(\cos\delta_c \cos\alpha_c) + \hat{y}_E(\cos\delta_c \sin\alpha_c) + \hat{z}_E \sin\delta_c \,. \tag{19}$$

The same vector can be referred to the geocentric system by direct application of Eqs. (12) and (14). We then have

$$(\hat{n})_G = \hat{x}_G \left[\cos\delta_c \cos(\tau_G - \alpha_c)\right] + \hat{y}_G \left[\cos\delta_c \sin(\tau_G - \alpha_c)\right] + \hat{z}_G \sin\delta_c \,. \tag{20}$$

The z axis of the camera system coincides with the optic axis. The unit vector $\hat{z}_c$ is therefore identical with the unit vector $\hat{n}$, and its geocentric representation is also given by Eq. (20).

When points at finite distances from the camera are observed, the general transformations must be used but knowledge of the orientation of the z axis of the camera system with respect to the geocentric system is prerequisite to the transformation. Consider the situation depicted in Figure 6. The geocentric coordinates are represented by nonsubscripted variables. Unit vectors associated with the camera system are identified by the subscript c. Their components are to be referred to the geocentric system. Let $\hat{c}$ be a unit vector along the line of sight to the point P. If the distance SP = a, then the vector $\overrightarrow{SP} = a\hat{c}$. The vector $\hat{c}$, referred to the camera system, can be written in the form

$$\hat{c} = p\hat{z}_c + q\hat{\nu}_c \,, \tag{21}$$

where

$$\hat{\nu}_c \cdot \hat{z}_c = 0 \,. \tag{22}$$

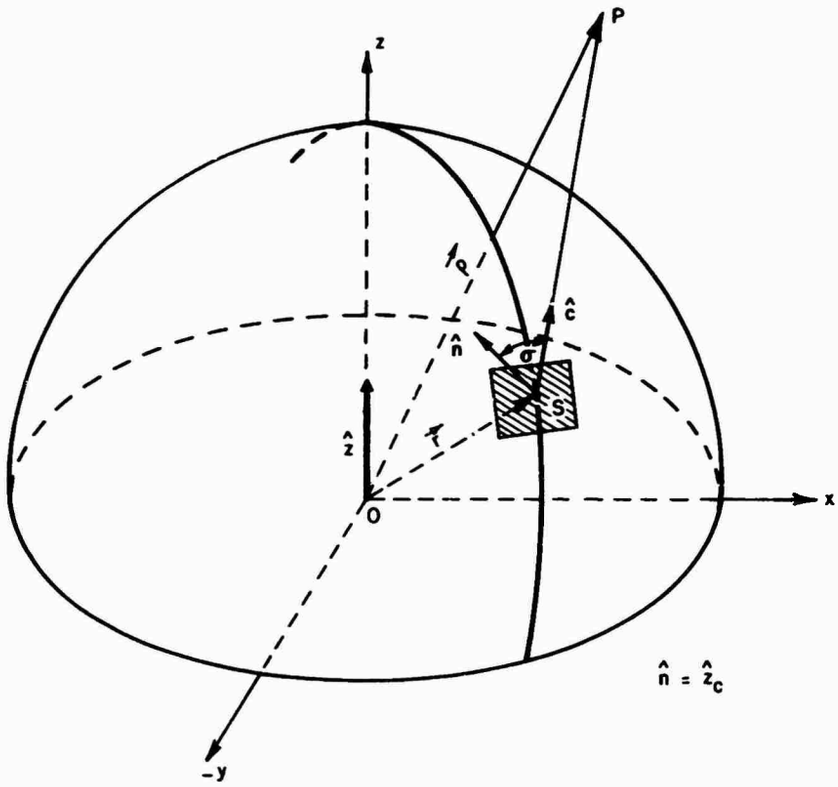

Figure 6. Relation Between Camera and Geocentric Systems

Clearly, the vector $\hat{\nu}_c$ is contained in the plane determined by the line of sight and the camera optic axis and, because of Eq. (22), is in the camera system xy plane.

Figure 7 represents a photograph of P. The fiducial marks determine plate axes from which the distances x' and y' are measured. For a rotation angle $\delta\epsilon = 0$, the plate axes coincide with the $x_c y_c$ axes, which define the E-W and N-S directions on the plate. Clearly, the unit vector $\hat{x}_c$, which points toward the east, is proportional to the vector product of $\hat{z}$ and $\hat{z}_c$, that is,

$$\hat{x}_c = \frac{\hat{z} \times \hat{z}_c}{|\hat{z} \times \hat{z}_c|} \quad . \tag{23}$$

If for simplicity we write Eq. (20) in the form

$$(\hat{n})_G = \hat{z}_c = \hat{x}n_1 + \hat{y}n_2 + \hat{z}n_3 \ , \tag{24}$$

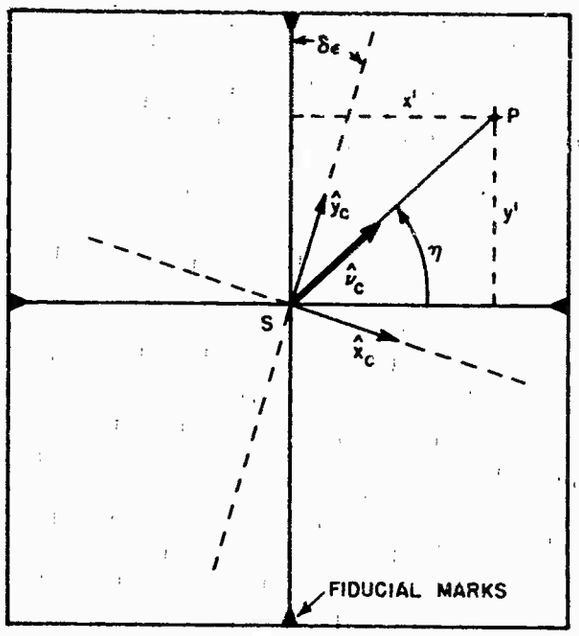

Figure 7. Coordinate Systems on the Film Plane

where

$$n_1 = \cos\delta_c \cos(\tau_G - \alpha_c) ,$$

$$n_2 = \cos\delta_c \sin(\tau_G - \alpha_c) ,$$

$$n_3 = \sin\delta_c ,$$

Eq. (23) becomes

$$\hat{x}_c = \frac{1}{\sqrt{n_1^2 + n_2^2}} \left(-\hat{x}n_2 + \hat{y}n_1\right) . \tag{25}$$

The unit vector along the third axis of the cartesian camera system, $\hat{y}_c$, is simply the vector product

$$\hat{y}_c = \hat{z}_c \times \hat{x}_c , \tag{26}$$

or, in component form,

$$\hat{y}_c = \frac{1}{\sqrt{n_1^2 + n_2^2}}\left[-\hat{x}(n_1 n_3) - \hat{y}(n_2 n_3) + \hat{z}(n_1^2 + n_2^2)\right]. \tag{27}$$

From Figure 7 it follows that

$$\hat{\nu}_c = \hat{x}_c \cos(\eta + \delta\epsilon) + \hat{y}_c \sin(\eta + \delta\epsilon) . \tag{28}$$

The vector $\hat{c}$, along the line of sight to the point P, is therefore

$$\begin{aligned}\hat{c} = \hat{x}&\left\{n_1 \cos\sigma - \frac{\sin\sigma}{\Delta}\left[n_2 \cos(\eta + \delta\epsilon) + n_1 n_3 \sin(\eta + \delta\epsilon)\right]\right\} + \\ &+ \hat{y}\left\{n_2 \cos\sigma + \frac{\sin\sigma}{\Delta}\left[n_1 \cos(\eta + \delta\epsilon) - n_2 n_3 \sin(\eta + \delta\epsilon)\right]\right\} + \\ &+ \hat{z}\left[n_3 \cos\sigma + \Delta \sin\sigma \sin(\eta + \delta\epsilon)\right] ,\end{aligned} \tag{29}$$

where

$$\Delta = \sqrt{n_1^2 + n_2^2} .$$

An alternative way of deriving this expression will now be given. Equations (24), (25), and (27) can be recognized as the columns of the matrix representing the purely rotational part of the coordinate transformation that takes us from a simplified camera system, for which the angle $\delta\epsilon = 0$, to the geocentric system. Written in full, this matrix is

$$R = \begin{pmatrix} -n_2/\Delta & -n_1 n_3/\Delta & n_1 \\ n_1/\Delta & n_2 n_3/\Delta & n_2 \\ 0 & \Delta & n_3 \end{pmatrix} . \tag{30}$$

Since det R = 1 and the matrix is real, the inverse transformation is effected by the transposed matrix

$$R^{-1} = R^T = \begin{pmatrix} -n_2/\Delta & n_1/\Delta & 0 \\ -n_1 n_3/\Delta & -n_2 n_3/\Delta & \Delta \\ n_1 & n_2 & n_3 \end{pmatrix} . \tag{31}$$

The matrix (30) can be obtained directly from Eq. (15) with $\delta\epsilon = 0$, and from Eq. (11) with $\theta = \tau_G$. Evidently,

$$\begin{aligned} R &= R_z(\tau_G)\, R_z^{-1}(\alpha_c)\, R_y^{-1}\left(\tfrac{\pi}{2} - \delta_c\right) \\ &= R_z(\tau_G - \alpha_c)\, R_y^{-1}\left(\tfrac{\pi}{2} - \delta_c\right) . \end{aligned} \tag{32}$$

The vector $\hat{c}$, as given by Eq. (29), is obtained by performing, in addition to the rotation R, a rotation about the z_c axis through the angle $-\delta\epsilon$. In other words,

$$\begin{pmatrix} c_x \\ c_y \\ c_z \end{pmatrix}_G = R_z(\tau_G - \alpha_c)\, R_y^{-1}\left(\tfrac{\pi}{2} - \delta_c\right) R_z(-\delta\epsilon) \begin{pmatrix} \cos\eta \sin\sigma \\ \sin\eta \sin\sigma \\ \cos\sigma \end{pmatrix} . \tag{33}$$

The vectorial derivation previously given serves to identify $\hat{x}_c$ and $\hat{y}_c$ as vectors that point east and north, respectively, but for routine computations with high-speed digital equipment, Eq. (33) is to be preferred. This is because it can be implemented by means of subroutines of general applicability in the triangulation procedure.

Having referred the unit vector along the line of sight to the geocentric system we are now able to write down the expression for the position vector $\overrightarrow{OP} = \vec{\rho}$. Clearly,

$$\vec{\rho} = \vec{r} + a\hat{c} , \tag{34}$$

where, we recall, $\vec{r}$ is the vector that fixes the position of the origin of the camera system at site S. It can be recognized that the addition of $\vec{r}$ to the vector $a\hat{c}$ corresponds to the translational part of the transformation that relates position measurements in the camera system to position measurements in the geocentric system. Later on we shall see how $\vec{r}$ is determined from geodetic data appropriate to the observation site. For the moment it suffices to assume that the vector $\vec{r}$ is

specified by its cartesian components

$$\vec{r} = r\hat{r} = x\hat{x} + y\hat{y} + z\hat{z}$$

$$= r\,(\hat{x}\cos\gamma_1 + \hat{y}\cos\gamma_2 + \hat{z}\cos\gamma_3)\,. \tag{35}$$

The direction cosines $\cos\gamma_i$ can be expressed as functions of the geocentric latitude ϕ' and the longitude λ. The following can easily be verified:

$$\begin{pmatrix} \cos\gamma_1 \\ \cos\gamma_2 \\ \cos\gamma_3 \end{pmatrix} = R_z^{-1}(-\lambda)\,R_z^{-1}\left(\frac{\pi}{2} - \phi'\right)\begin{pmatrix} 0 \\ 0 \\ 1 \end{pmatrix} = \begin{pmatrix} \cos\lambda\cos\phi' \\ \sin\lambda\cos\phi' \\ \sin\phi' \end{pmatrix}. \tag{36}$$

Equation (36) is consistent with the convention that western longitudes and southern latitudes are negative.

Equations (20), (29), and (34) solve the problem of expressing in terms of geocentric coordinates the position of a point at a finite distance from a triangulation site whose position and orientation are known. In Sec. 4 we discuss the means to determine that orientation.

4. ORIENTATION OF THE CAMERA SYSTEM

Equation (15) relates the right ascension and declination of a star to the angular coordinates σ and η that correspond to the orientation, in the camera system, of the line of sight to the star. The transformation (15) depends on three parameters, of which α_c and δ_c are identified as the right ascension and declination of the point on the celestial sphere toward which the camera optic axis is directed, and $\delta\epsilon$ corresponds to a rotation of the film plane about the optic axis.

We will now set up a procedure to determine α_c, δ_c, and $\delta\epsilon$ from photographic records of stars. Properly identified by comparison with charts from a star atlas, they will supply the data from which the column vectors on the righthand side of Eq. (15) can be constructed. Measurements of the corresponding star images on the film will provide the data that, coupled with Eqs. (5), (6), and (7), will allow evaluation of the components of the column vectors on the lefthand side of Eq. (6). Since the position of each star can be described by only two independent equations involving its right ascension and declination, identification of a single

star is not sufficient to solve for the three unknowns α_c, δ_c, and $\delta\epsilon$. From photographs of a single star we can find the values of only two unknowns. For example, if we take $\delta\epsilon = 0$, we are led to Eqs. (17 a, b, c). We can readily verify the validity of the following expressions for α_c and δ_c:

$$\alpha_c = \alpha - \sin^{-1}\left(\frac{\sin\eta \sin\sigma}{\cos\delta}\right), \tag{37}$$

$$\delta_c = \sin^{-1}\left(\frac{\sin\delta}{\sqrt{1-\sin^2\sigma \sin^2\eta}}\right) + \tan^{-1}(\cos\eta \tan\sigma). \tag{38}$$

For the general case we have to consider the full set of equations arising from Eq. (15) together with data from at least two stars. We have:

$$\cos\delta\epsilon\left[\sin\delta_c \cos\delta \cos(\alpha_c-\alpha) - \cos\delta_c \sin\delta\right] - \sin\delta\epsilon \cos\delta \sin(\alpha_c - \alpha) = \cos\eta \sin\sigma, \tag{39a}$$

$$\sin\delta\epsilon\left[\sin\delta_c \cos\delta \cos(\alpha_c-\alpha) - \cos\delta_c \sin\delta\right] + \cos\delta\epsilon \cos\delta \sin(\alpha_c-\alpha) = -\sin\eta \sin\sigma, \tag{39b}$$

$$\cos\delta_c \cos\delta \cos(\alpha_c-\alpha) + \sin\delta_c \sin\delta = \cos\sigma. \tag{39c}$$

Equations (39) can be written in the equivalent form

$$\cos\delta \sin(\alpha_c-\alpha) + \sin\sigma \sin(\eta + \delta\epsilon) = 0, \tag{40a}$$

$$\sin\delta_c \cos\delta \cos(\alpha_c-\alpha) - \cos\delta_c \sin\delta = \sin\sigma \cos(\eta + \delta\epsilon), \tag{40b}$$

$$\cos\delta_c \cos\delta \cos(\alpha_c-\alpha) + \sin\delta_c \sin\delta = \cos\sigma. \tag{40c}$$

The added rotation of the film plane about the optic axis appears as a correction in the angle η, which measures the azimuth of the star image from the reference direction determined by the fiducial marks.

Equations (40b) and (40c) can be used to express $\sin\delta_c$ and $\cos\delta_c$ as functions of α_c and $\delta\epsilon$. It can readily be seen that

$$\sin\delta_c = \frac{1}{2\Delta_1}\left[\sin 2\delta \cos(\alpha_c - \alpha) + \sin 2\sigma \cos(\eta + \delta\epsilon)\right]$$

$$= \frac{1}{\Delta_2}\left[\sin\delta \cos\sigma + \cos\delta \sin\sigma \cos(\eta + \delta\epsilon) \cos(\alpha_c - \alpha)\right], \tag{41a}$$

$$\cos\delta_c = \frac{1}{2\Delta_1}\left[\cos 2\delta + \cos 2\sigma\right] = \frac{1}{\Delta_2}\left[\cos\delta \cos\sigma \cos(\alpha_c - \alpha) - \right.$$

$$\left. - \sin\delta \sin\sigma \cos(\eta + \delta\epsilon)\right], \tag{41b}$$

where

$$\Delta_1 = \cos\sigma \cos\delta \cos(\alpha_c - \alpha) + \sin\sigma \sin\delta \cos(\eta + \delta\epsilon),$$

$$\Delta_2 = 1 - \cos^2\delta \sin^2(\alpha_c - \alpha). \tag{41c}$$

Consequently,

$$\tan\delta_c = \frac{\sin 2\delta \cos(\alpha_c - \alpha) + \sin 2\sigma \cos(\eta + \delta\epsilon)}{\cos 2\delta + \cos 2\sigma}$$

$$= \frac{\sin\delta \cos\sigma + \cos\delta \sin\sigma \cos(\eta + \delta\epsilon) \cos(\alpha_c - \alpha)}{\cos\delta \cos\sigma \cos(\alpha_c - \alpha) - \sin\delta \sin\sigma \cos(\eta + \delta\epsilon)}. \tag{42}$$

We now consider Eq. (40a), rewritten in the form

$$\sin\alpha_c \cos\delta \cos\alpha - \cos\alpha_c \cos\delta \sin\alpha = -\sin\sigma \sin(\eta + \delta\epsilon). \tag{43}$$

Then we evaluate Eq. (43) for each of two stars and solve for $\sin\alpha_c$ and $\cos\alpha_c$. With the subscripts 1 and 2 corresponding to the first and second stars, respectively, we have

$$\sin\alpha_c = \frac{\sin u_2 \sin\alpha_1 - \sin u_1 \sin\alpha_2}{\sin(\alpha_1 - \alpha_2)} \tag{44a}$$

$$\cos\alpha_c = \frac{\sin u_2 \cos\alpha_1 - \sin u_1 \cos\alpha_2}{\sin(\alpha_1 - \alpha_2)}, \tag{44b}$$

where

$$\sin u_i = -\left(\frac{\sin\sigma_i}{\cos\delta_i}\right) \sin(\eta_i + \delta\epsilon). \tag{44c}$$

By virtue of the identity $\sin^2 \alpha_c + \cos^2 \alpha_c = 1$, we can write

$$\sin^2 (\alpha_1 - \alpha_2) = \sin^2 u_1 + \sin^2 u_2 - 2 \sin u_1 \sin u_2 \cos (\alpha_1 - \alpha_2) .$$

But

$$\sin^2 u_i = \frac{1}{2} \left(\frac{\sin \sigma_i}{\cos \delta_i}\right)^2 \left(1 - \cos 2\eta_i \cos 2\delta\epsilon + \sin 2\eta_i \sin 2\delta\epsilon \right) ,$$

and

$$\sin u_1 \sin u_2 = \frac{1}{2} \left(\frac{\sin \sigma_1}{\cos \delta_1}\right)\left(\frac{\sin \sigma_2}{\cos \delta_2}\right)\Big[\cos (\eta_1 - \eta_2) - \cos 2\delta\epsilon \cos (\eta_1 + \eta_2) + \\ + \sin 2\delta\epsilon \sin (\eta_1 + \eta_2)\Big] .$$

Consequently, we can write

$$S_1 \cos 2\delta\epsilon - S_2 \sin 2\delta\epsilon = S_o , \tag{45}$$

where

$$S_1 = \cos 2\eta_1 \left(\frac{\sin \sigma_1}{\cos \delta_1}\right)^2 - 2\left(\frac{\sin \sigma_1}{\cos \delta_1}\right)\left(\frac{\sin \sigma_2}{\cos \delta_2}\right) \cos (\eta_1 + \eta_2) \cos (\alpha_1 - \alpha_2) + \\ + \left(\frac{\sin \sigma_2}{\cos \delta_2}\right)^2 \cos 2\eta_2 ,$$

$$S_2 = \sin 2\eta_1 \left(\frac{\sin \sigma_1}{\cos \delta_1}\right)^2 - 2\left(\frac{\sin \sigma_1}{\cos \delta_1}\right)\left(\frac{\sin \sigma_2}{\cos \delta_2}\right) \sin (\eta_1 + \eta_2) \cos (\alpha_1 - \alpha_2) + \\ + \left(\frac{\sin \sigma_2}{\cos \delta_2}\right)^2 \cos 2\eta_2 ,$$

$$S_o = \left(\frac{\sin \sigma_1}{\cos \delta_1}\right)^2 - 2\left(\frac{\sin \sigma_1}{\cos \delta_1}\right)\left(\frac{\sin \sigma_2}{\cos \delta_2}\right) \cos (\alpha_1 \ \alpha_2) + \left(\frac{\sin \sigma_2}{\cos \ _2}\right)^2 - \\ - 2 \sin^2 (\alpha_1 - \alpha_2) .$$

From Eq. (45) it follows that

$$\cos (2\delta\epsilon + \psi) = \frac{S_o}{\sqrt{S_1^2 + S_2^2}} ,$$

with

$$\psi = \tan^{-1} \frac{S_2}{S_1} .$$

From this equation we find the following expressions for $\delta\epsilon$:

$$\delta\epsilon = \frac{1}{2}\left(\cos^{-1} \frac{S_o}{\sqrt{S_1^2 + S_2^2}} - \tan^{-1} \frac{S_2}{S_1}\right)$$

$$= \frac{1}{2} \cos^{-1}\left[\frac{\frac{S_1}{S_o} + \frac{S_2}{S_o}\sqrt{\left(\frac{S_1}{S_o}\right)^2 + \left(\frac{S_2}{S_o}\right)^2 - 1}}{\frac{S_1^2}{S_o} + \frac{S_2^2}{S_o}}\right]$$

$$= \frac{1}{2} \tan^{-1}\left[\frac{\sqrt{\left(\frac{S_1}{S_o}\right)^2 + \left(\frac{S_2}{S_o}\right)^2 - 1} - \frac{S_2}{S_1}}{1 + \frac{S_2}{S_1}\sqrt{\left(\frac{S_1}{S_o}\right)^2 + \left(\frac{S_2}{S_o}\right)^2 - 1}}\right] . \tag{46}$$

From Eqs. (46) it is apparent that the rotation angle $\delta\epsilon$ vanishes for $S_1 = S_o$. This leads to the condition

$$\left(\frac{\sin\sigma_1 \sin\eta_1}{\cos\delta_1} - \frac{\sin\sigma_2 \sin\eta_2}{\cos\delta_2}\right)^2 = 2\left(\frac{\sin\sigma_1}{\cos\delta_1}\right)\left(\frac{\sin\sigma_2}{\cos\delta_2}\right)\left[\cos(\alpha_1 - \alpha_2) \times\right.$$

$$\left. \times \sin^2 \frac{\eta_1 + \eta_2}{2} - \sin\eta_1 \sin\eta_2\right] + \sin^2(\alpha_1 - \alpha_2) ,$$

which can be used in conjunction with Eqs. (37) and (38) to check the consistency of the data from pairs of stars for known $\delta\epsilon = 0$.

Having determined the angle $\delta\epsilon$, which measures the rotation of the xy plane of the camera system from the N-S direction, we can use Eqs. (44) and (42) to find the angles α_c and δ_c that identify the orientation of the optic axis (or, equivalently, the orientation of the camera system z axis). We have

$$\tan \alpha_c = \frac{\sin u_2 \sin \alpha_1 - \sin u_1 \sin \alpha_2}{\sin u_2 \cos \alpha_1 - \sin u_1 \cos \alpha_2} \tag{47}$$

and

$$\tan \delta_c = \frac{\sin 2\delta \cos (\alpha_c - \alpha) + \sin 2\sigma \cos (\eta + \delta\epsilon)}{\cos 2\delta + \cos 2\sigma} , \tag{48}$$

where, as before,

$$\sin u_i = -\left(\frac{\sin \sigma_i}{\cos \delta_i}\right) \sin (\eta_i + \delta\epsilon) .$$

Note that Eq. (47) uses data from star pairs whereas Eq. (48) refers to a single star. It is possible to write expressions for $\tan \delta_c$ that also use data from two stars. One such expression is

$$\tan \delta_c = \frac{\cos \sigma_1 \cos \delta_2 \cos (\alpha_c - \alpha_2) - \cos \sigma_2 \cos \delta_1 \cos (\alpha_c - \alpha_1)}{\cos \sigma_1 \sin \delta_2 - \cos \sigma_2 \sin \delta_1} \tag{49}$$

It should be remarked that the statements made at the outset concerning the need to use data from at least a pair of stars in order to evaluate the angles α_c, δ_c, and $\delta\epsilon$ is fully consistent with the system of Eqs. (40). We have here three equations, which in ordinary circumstances should be sufficient to solve for the three unknowns. Closer examination, however, discloses that they are not independent. Unless previous information is available about the value of any one of the unknowns, a sufficient number of independent equations can only be obtained by adjoining to the set of equations from one star the corresponding set for a second star.

5. TRIANGULATION PROCEDURE FOR POINT RELEASES

Consider now the problem of determining the geocentric coordinates of the point in space that marks the position of a chemical puff. To locate the puff, photographs are taken from two or more stations whose geodetic coordinates are known. Let us assume that the geocentric coordinates of the stations have been found by an appropriate transformation.* Construct the position vectors $\vec{r}_i$ that fix the location of the stations in the geocentric system. They have the general form specified by Eqs. (3) and (4), that is,

* This transformation is discussed in Sec. 7.

$$\vec{r}_i = r_i \hat{g}_i ,$$

where

$$\hat{g}_i = \hat{x}\,(\cos\lambda_i \cos\phi_i') + \hat{y}\,(\sin\lambda_i \cos\phi_i') + \hat{z}\,\sin\phi_i' ,$$

and ϕ_i', λ_i denote the geocentric latitude and longitude of the ith station. At each observation site a camera is mounted with its axis oriented in a direction specified by the unit vector $\hat{n}$, whose geocentric components were determined in Sec. 3, Eq. (20), such that

$$\hat{n} = \hat{x} \cos\delta_c \cos(\tau_G - \alpha_c) + \hat{y} \cos\delta_c \sin(\tau_G - \alpha_c) + \hat{z} \sin\delta_c .$$

There will be one such $\hat{n}$ vector for each coordinate system associated with a camera. To avoid an overabundance of subscripts this equation shows the general form of $\hat{n}$. When it becomes necessary to identify a particular $\hat{n}$, we will attach the subscript and write $\hat{n}_i$. The expanded form for $\hat{n}_i$ is computed from the α_c, δ_c, and τ_G appropriate to the camera and observation site under discussion.

Let us now consider the situation depicted in Figure 8. A point release at P is photographed from sites S_1 and S_2. It was shown in Sec. 3 that along the line of sight, a unit vector $\hat{c}$ is expressed in geocentric coordinates by Eq. (29), repeated here for convenience:

$$\begin{aligned}\hat{c} = {} & \hat{x}\left\{ n_1 \cos\sigma - \frac{\sin\sigma}{\Delta}\left[n_2 \cos(\eta + \delta\epsilon) + n_1 n_3 \sin(\eta + \delta\epsilon)\right]\right\} + \\ & + \hat{y}\left\{ n_2 \cos\sigma + \frac{\sin\sigma}{\Delta}\left[n_1 \cos(\eta + \delta\epsilon) - n_2 n_3 \sin(\eta + \delta\epsilon)\right]\right\} + \\ & + \hat{z}\left[n_3 \cos\sigma + \Delta \sin\sigma \sin(\eta + \delta\epsilon)\right] ,\end{aligned} \qquad [(29)]$$

where

$$\Delta = \sqrt{n_1^2 + n_2^2} .$$

Let us introduce the notation:

$$\overrightarrow{OP} = \vec{\rho}$$

$$\overrightarrow{OS}_1 = \vec{r}_1$$

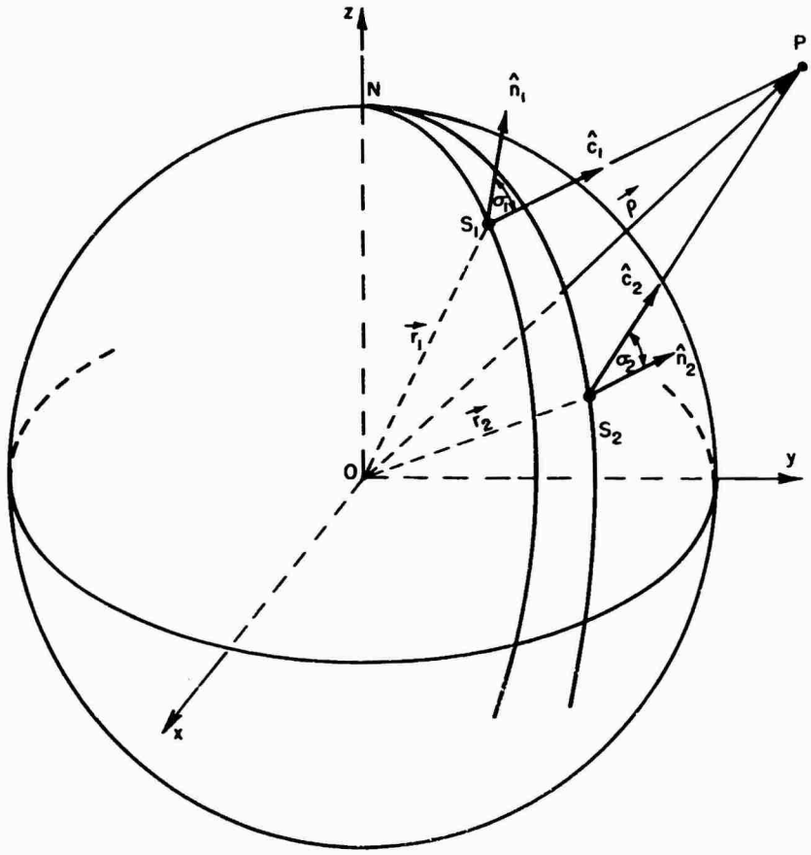

Figure 8. Triangulation on Point Releases

$$\overrightarrow{OS_2} = \vec{r}_2$$

$$\overrightarrow{S_1P} = a\hat{c}_1$$

$$\overrightarrow{S_2P} = b\hat{c}_2$$

$$\overrightarrow{S_1S_2} = \vec{d}$$

The triangulation problem consists of finding an expression for the vector $\vec{\rho}$. From Figure 8 it is evident that we can write

$$\vec{\rho} = \vec{r}_1 + a\hat{c}_1 , \tag{50a}$$

$$\vec{\rho} = \vec{r}_2 + b\hat{c}_2 . \tag{50b}$$

By a scalar multiplication of Eqs. (50a) and (50b) we obtain for the magnitude of $\vec{\rho}$ the expression

$$\rho = \left(\vec{r}_i \cdot \vec{r}_2 + a\vec{r}_2 \cdot \hat{c}_1 + b\vec{r}_1 \cdot \hat{c}_2 + ab\, \hat{c}_1 \cdot \hat{c}_2\right)^{1/2} . \tag{51}$$

Vector multiplication leads to the relation:

$$0 = \vec{\rho} \times \vec{\rho} = \vec{r}_1 \times \vec{r}_2 + a(\hat{c}_1 \times \vec{r}_2) + b(\vec{r}_1 \times \hat{c}_2) + ab(\hat{c}_1 \times \hat{c}_2) . \tag{52}$$

Take now the scalar product of Eq. (52) and $\hat{c}_1$ or $\hat{c}_2$. This procedure leads to the following explicit expressions for the scale factors a and b:

$$a = \frac{\hat{c}_2 \cdot \vec{r}_1 \times \vec{r}_2}{\vec{r}_2 \cdot \hat{c}_1 \times \hat{c}_2} = - \frac{\vec{r}_1 \cdot \vec{r}_2 \times \hat{c}_2}{\hat{c}_1 \cdot \vec{r}_2 \times \hat{c}_2} , \tag{53a}$$

$$b = \frac{\hat{c}_1 \cdot \vec{r}_1 \times \vec{r}_2}{\vec{r}_1 \cdot \hat{c}_1 \times \hat{c}_2} = - \frac{\vec{r}_2 \cdot \vec{r}_1 \times \hat{c}_1}{\hat{c}_2 \cdot \vec{r}_1 \times \hat{c}_1} . \tag{53b}$$

The consistency of the scheme can be checked by virtue of the relation

$$\vec{d} \cdot \vec{d} = d^2 = (b\hat{c}_2 - a\hat{c}_1)^2 = a^2 + b^2 - 2ab\,(\hat{c}_1 \cdot \hat{c}_2) , \tag{54}$$

in which d^2 represents the square of the distance separating the two observation sites. This distance is often directly available, having been ascertained when the region where the observation sites are located was surveyed. Alternative expressions for the position vector $\vec{\rho}$ are obtained when values of a and b are substituted in Eqs. (50a) and (50b). Since there is no a priori reason to favor one observation site over the other, it is advisable to define $\vec{\rho}$ as a symmetric combination of Eqs. (50a) and (50b), that is,

$$\vec{\rho} = \frac{1}{2}\left(\vec{r}_1 + \vec{r}_2 + a\hat{c}_1 + b\hat{c}_2\right) . \tag{55}$$

In combination with Eq. (51) this expression can be used to define a unit vector $\hat{\rho}$ in the direction of OP, the position vector of the release. Knowledge of this unit vector allows immediate calculation of the geocentric latitude of the release. Clearly,

$$\hat{\rho} \cdot \hat{z} = \cos\left(\frac{\pi}{2} - \phi'_p\right) \sin \phi'_p , \tag{56}$$

where ϕ'_p denotes the geocentric latitude of P. Similarly, the longitude λ_p of the release point can be computed from the expression

$$\tan \lambda_p = \frac{\vec{\rho} \cdot \hat{y}}{\hat{\rho} \cdot \hat{x}} . \tag{57}$$

If only the cartesian geocentric coordinates of the point P are required, Eq. (55) is all that is needed. Equations (51), (56), and (57) allow parametrization of these components, thus serving to locate P in the geocentric system by means of spherical coordinates. This is particularly useful because geodetic coordinates can be obtained from this form very readily. [The transformation formulas will be discussed in Sec. 7.]

The position vector $\vec{\rho}$, which locates the point P in the geocentric frame of reference, is uniquely determined when independent observations from two or more stations are available. Equations (55) and (53a, b) solve the two-station problem. It can easily be shown that for N stations the position vector $\vec{\rho}$ is given by the expression:

$$\vec{\rho} = \frac{1}{N} \sum_{J=1}^{N} \left(\vec{r}_j + a_j \hat{c}_j \right), \tag{58}$$

where

$\vec{r}_j$ = position vector of jth camera site

$\hat{c}_j$ = unit vector along the direction of the jth camera optic axis

a_j = scale factors for the jth line of sight, given by the vector relations

$$a_j = - \frac{\vec{r}_j \cdot \sum_{i=1}^{N} \vec{r}_i \times \hat{c}_i}{\hat{c}_j \cdot \sum_{i=1}^{N} \vec{r}_i \times \hat{c}_i} . \tag{59}$$

There is some arbitrariness in the construction of a check equation similar to Equation (54) for the two-station case. A symmetric form can be built by taking the stations in a close cycle and computing

$$\sum_{i=1}^{N} d_{i,i+1}^2 = 2\sum_{i=1}^{N} a_i^2 - 2\sum_{i=1}^{N} a_i a_{i+1}\left(\hat{c}_i \cdot \hat{c}_{i+1}\right), \tag{60}$$

where the index N+1 is to be identified with the index 1, a condition necessary to complete an arbitrary closed cycle of stations with no cross links.

Before concluding this section a reminder is in order about the significance of Eqs. (58) and (59). It has been implicit that the analysis that led to Eq. (59) assumes that all lines of sight intersect at the point P, which coincides with some structural feature of the release uniquely identifiable from all observation sites. Then, Eq. (58) represents the position vector obtained by making use of all observations symmetrically, with equal weights. In a sense, it is a mean value of equally weighted observations. The more interesting, but more involved problem of deriving expressions for the probable error and standard deviation associated with the mean value given by Eq. (58) will be the subject of a separate report. Thus, the simplicity of our approach is revealed at all stages, unencumbered by the complexities of a full statistical analysis.

6. TRIANGULATION ON CONTINUOUS TRAILS

For the triangulation scheme that was discussed in Sec. 5 it is assumed that the images of a distinct cloud feature can be individually identified on photographs from different sites. This is not possible when the chemical release takes the form of a continuous trail. For example, from a pair of observation sites the two trail images have the general appearance shown in Figure 9. This figure clearly indicates that, except possibly for the trail end, it is not usually possible to establish a unique correspondence between a given point P_1 on trail image 1 and some point P_2 on trail image 2.

To match point pairs on the two trails it is necessary to use a more general computational scheme for the triangulation, one that allows the position of point P_2 along the second trail image to be varied until some criterion for optimum match is satisfied. This requires a procedure for moving along the trail image and scanning over short sections of it to locate the optimum pairing. A very convenient way to accomplish this is to replace the actual trail image by a two-dimensional curve, which is represented analytically by a parametric cubic spline (Ahlberg, Nilson, and Walsh, 1967). For computer implementation, the scan can be effected by systematically incrementing the spline parameter. The merit function that measures the quality of the match is computed after each increment. In general, it will decrease as the scan proceeds, reach a minimum, and then increase

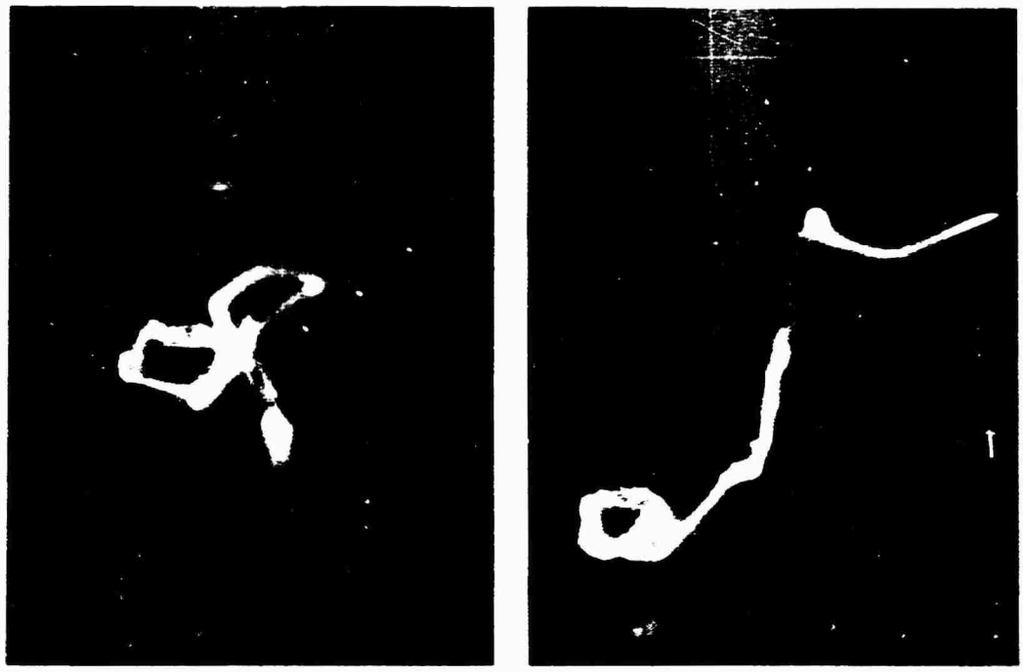

Figure 9. Luminescent Trail as Observed From Two Different Triangulation Sites

(Bekey and McGhee, 1964). If the increments are small enough, or if suitable interpolation procedures are used, the minimum value can be determined very precisely.

It is not the purpose of this report to dwell on this aspect of the triangulation problem. Rather, let us try to establish the analytic form of the merit function and assume that adequate procedures are available for an effective determination of the optimum match.

Consider, then, the situation depicted in Figure 10. The vector diagram shows the essential geometry involved. Clearly,

$$\vec{d} = \vec{r}_1 - \vec{r}_2 = d\hat{d} \tag{61}$$

and

$$a\hat{c}_1 - \vec{s} - b\hat{c}_2 + d\hat{d} = 0 \, . \tag{62}$$

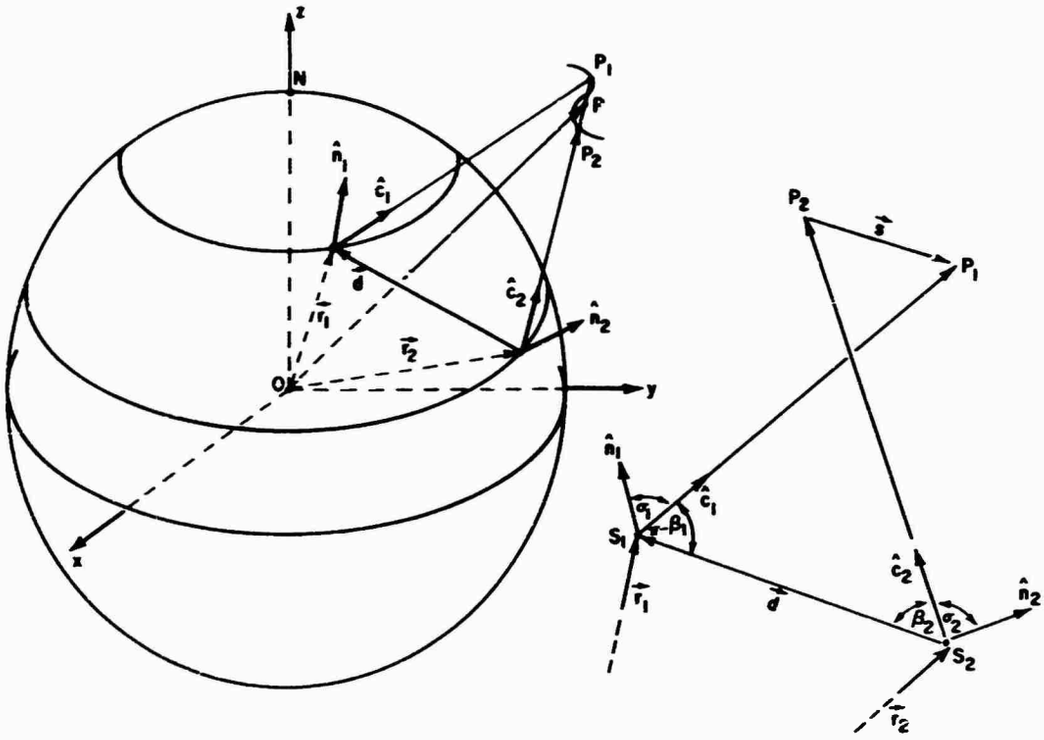

Figure 10. Triangulation on Trails

To determine the scale factors a and b we define $s = |\vec{s}|$ as the minimum distance between the lines of sight. We can then write

$$\vec{s} = d\hat{d} + a\hat{c}_1 - b\hat{c}_2 , \tag{63a}$$

$$\vec{s}\cdot\hat{c}_1 = \vec{s}\cdot\hat{c}_2 = 0 , \tag{63b}$$

whence we obtain the following expressions for a and b

$$a = -d\left[\frac{\hat{d}\cdot\hat{c}_1 - (\hat{d}\cdot\hat{c}_2)(\hat{c}_1\cdot\hat{c}_2)}{1 + (\hat{c}_1\cdot\hat{c}_2)^2}\right] , \tag{64}$$

$$b = d\left[\frac{\hat{d}\cdot\hat{c}_2 - (\hat{d}\cdot\hat{c}_1)(\hat{c}_1\cdot\hat{c}_2)}{1 + (\hat{c}_1\cdot\hat{c}_2)^2}\right] . \tag{65}$$

A vector $\vec{\rho}$ can now be constructed from the origin to the midpoint of the line segment P_1P_2. By virtue of conditions (63b), P_1P_2 is the shortest distance between the lines of sight and, clearly,

$$\vec{\rho} = \vec{r}_1 + a\hat{c}_1 - \frac{1}{2}\vec{s} ,$$

$$\vec{\rho} = \vec{r}_2 + b\hat{c}_2 + \frac{1}{2}\vec{s} .$$

Consequently,

$$\vec{\rho} = \frac{1}{2}\left(\vec{r}_1 + \vec{r}_2 + a\hat{c}_1 + b\hat{c}_2\right) . \tag{66}$$

Equation (66) is identical with Eq. (55), which was obtained for point releases. The disappearance of any reference to $\vec{s}$ in Eq. (66) indicates that the role of $\vec{s}$ is to supply a quantitative measure of the closure error incurred when the lines of sight and the base line connecting the observation sites are taken as the sides of a triangle with one vertex marking the release point. For point releases, any discrepancy between the left- and righthand sides of Eq. (54) serves to characterize this closure error. By modifying the procedure used to evaluate a and b, it can easily be verified that Eqs. (64) and (65) can be obtained for point releases. In fact, these equations emerge instead of Eqs. (53a) and (53b) if the evaluation of a and b is based on the triangle S_1S_2P.

The closure error reduces to zero whenever the lines of sight intersect; however, the occurrence of intersecting lines of sight does not mean intersection at the point where the release has taken place. To estimate how far away from the actual release point the intersection occurs it is necessary to have data from more than two observation sites. The statistics of the $\vec{\rho}$ vectors will be discussed in a separate report.

Within the limitations imposed by triangulation from two sites, we now construct the function that allows matching points on pairs of trail images. Let us define the unit vectors $\hat{v}_1$ and $\hat{v}_2$ as follows:

$$\hat{v}_1 = \frac{\hat{d} \times \hat{c}_1}{\sin\beta_1} , \tag{67a}$$

$$\hat{v}_2 = \frac{\hat{d} \times \hat{c}_2}{\sin\beta_2} , \tag{67b}$$

where $\hat{v}_1$ is a vector normal to the plane determined by the lines S_1S_2 and S_1P_1, $\hat{v}_2$ is normal to the plane determined by lines S_1S_2 and S_2P_2, and $\sin\beta_i$ is the magnitude of the vector product $\hat{d} \times \hat{c}_i$. It is evident that if the two points P_1 and P_2 are images of the same trail point, the two planes coalesce and the vectors $\hat{v}_1$ and $\hat{v}_2$ are parallel. When this occurs, $1 - \hat{v}_1 \cdot \hat{v}_2$ vanishes. We can therefore make the function

$$f\left[\hat{c}_1, \hat{c}_2(t)\right] = 1 - \frac{\hat{c}_1 \cdot \hat{c}_2 - (\hat{d} \cdot \hat{c}_1)(\hat{d} \cdot \hat{c}_2)}{\sqrt{\left[1 - (\hat{d} \cdot \hat{c}_1)^2\right]\left[1 - (\hat{d} \cdot \hat{c}_2)^2\right]}} \tag{68}$$

the merit function that measures how close to coincidence the planes $S_1S_2P_1$ and $S_1S_2P_2$ come. Ideally, this function vanishes when P_2 becomes the second-site image of P_1. In practice, small residuals will almost always be present, and the criterion for a second-site match must be the occurrence of a minimum of $f\left[\hat{c}_1, \hat{c}_2(t)\right]$ as the parameter t is varied. This parameter determines the position of the point P_2 along the trail image.

It is clearly advantageous to have an analytic expression to describe the trail. In a perfectly still atmosphere, the trail centerline will coincide with the trajectory of the rocket that effects the release. In principle, it should be possible to write analytic expressions for this trajectory and, by suitable projective transformations, arrive at an equation for the trail centerline on the film plane. Besides the algebraic complexity that can be expected in all but a few special cases, there are considerations of winds, windshears, and turbulent transport processes that distort the trail and often create sharp twisting and self-intersections, the net result being that the analytic approach suggested by the static atmosphere model loses all significance.

The obvious way out of this difficulty is to employ a piecewise analytic representation of the trail centerline image. Since we have selected a parametric cubic spline representation, the ordinary treatment, which requires that the dependent variable be a single-valued function of the independent variable, has to be modified to allow for the multivaluedness introduced by severe twisting and self-intersections. An account of the parametric spline procedure is found in Appendix A.

Equations (64), (65), and (66) solve the triangulation problem for trails when observations are made from two stations. As was the case for triangulation on point releases, it is possible to extend the analysis and develop generalized expressions for the N-station case. If the position vector $\vec{\rho}$ is computed from the equation

$$\vec{\rho} = \frac{1}{N} \sum_{J=1}^{N} (\vec{r}_j + a_j \hat{c}_j) , \tag{69a}$$

it can be shown that the scale factors a_j are given by the relations

$$a_j = \left(f_j - \sum_{i=1}^{N} \frac{f_j - f_i}{Q_i} \right) \frac{1}{Q_j} , \tag{69b}$$

where

$$Q_i = \sum_{k=1}^{N} \hat{c}_i \cdot \hat{c}_k , \tag{70a}$$

$$f_i = \sum_{k=1}^{N} d_{ik} (\hat{d}_{ik} \cdot \hat{c}_k) . \tag{70b}$$

The vectors $\hat{c}_i$ are the unit vectors along the lines of sight that were introduced in Sec. 3. The vectors $\hat{d}_{ik}$ are unit vectors along the directed line from the ith to the kth station. The distance between these stations is d_{ik}. Clearly,

$$d_{ij} = d_{ji} ,$$

but

$$\hat{d}_{ij} = - \hat{d}_{ji} .$$

To match points on the trail images taken from the different triangulation sites it is necessary to construct a set of merit functions of the form (68). If a point is selected on the trail image corresponding to the ith station, the spline parameter values on the other images are determined by minimizing, in succession, the functions

$$f_{ij} \left[\hat{c}_i, \hat{c}_j(t_i^j) \right] = 1 - \frac{\hat{c}_i \cdot \hat{c}_j - (\hat{c}_i \cdot \hat{d}_{ij}) (\hat{c}_j \cdot \hat{d}_{ij})}{\sqrt{\left[1 - (\hat{c}_i \cdot \hat{d}_{ij})^2 \right] \left[1 - (\hat{c}_j \cdot \hat{d}_{ij})^2 \right]}} , \tag{71}$$

where t_j^i denotes the parameter for the jth trail image when the point to be matched lies on the ith trail image. The set of parameter values that is thus obtained is used to determine corresponding points on the N-1 trail images that have been compared with the ith image. It is not difficult to see that by successively

applying the same procedure to each trail—taking as the point to be matched the point on the trail determined by the parameter value that emerged from the initial round—a set of parameter values is obtained for each trail image, from which a mean value can be extracted, namely,

$$\langle t_j \rangle = \frac{1}{N} \sum_{k=1}^{N} t_j^k \, . \tag{72}$$

These averages can clearly be used to advantage to compute the line-of-sight unit vectors c_j that appear in Eqs. (69a) and (70). Higher moments of the distributions for the parameters t_j will be given elsewhere. The equations developed in this section, together with those of Sec. 5, solve the triangulation problems encountered in the course of reducing data from a chemical release. They lead to expressions for the geocentric coordinates of the release, from which such things as wind speeds are computed. To facilitate comparisons with existing data it is sometimes convenient to express positions as sets of coordinates relative to other systems of reference. Two of these will be discussed in Sec. 7.

7. TRANSFORMATIONS TO OTHER REFERENCE SYSTEMS

Although the equations developed in Secs. 5 and 6 solve the problem of establishing the position of chemical releases, these equations refer coordinates to a geocentric system. Some limitations that are thus imposed can only be resolved if means are provided to convert the coordinates to other reference systems. Two such systems (Kaula, 1966; Mueller, 1969) are discussed in this section: (1) the horizon system, which facilitates visualization of the release location with respect to the observer, (2) the geodetic system, which simplifies reference to geodetic or geographic charts. Since the transformations to and from these systems can be found without difficulty by applying the appropriate definitions or the rotation/translation operators introduced in Sec. 3, the transformations will be discussed with a minimum of detail concerning their derivation.

7.1 Geodetic Coordinates

Geodetic coordinates are defined with respect to a reference ellipsoid, a two-parameter surface of revolution very close to the actual surface of the earth. Geometrically, it is a quadric surface on which all curves of intersection with planes are either circles or ellipses. The ellipsoid is customarily defined by the length of the longest and shortest axes a and b, or, equivalently, by the long

axis a and one of the following auxiliary quantities

Flattening: $f = \frac{a - b}{a}$

First eccentricity: $\epsilon = \sqrt{1 - (b/a)^2}$

Second eccentricity: $\epsilon' = \sqrt{(a/b)^2 - 1}$

The ellipses whose generating planes contain the axis of rotation are the geodetic meridians. One of the geodetic meridians is selected as the zero meridian. The angle λ between the plane of the zero meridian and the plane of the geodetic meridian of a point P is the geodetic longitude of P. Clearly, if the zero meridian is contained in the plane of the geocentric prime meridian (Greenwich), the geodetic and geocentric longitudes are identical. The line PP' (see Figure 11) perpendicular to the tangent plane at the point where PP' pierces the ellipsoid is a geodetic normal. The angle ϕ between this normal and a plane perpendicular to the axis of rotation (for example, the geodetic equator) is the geodetic latitude of P. Figure 11 also shows the corresponding geocentric latitude ϕ'.

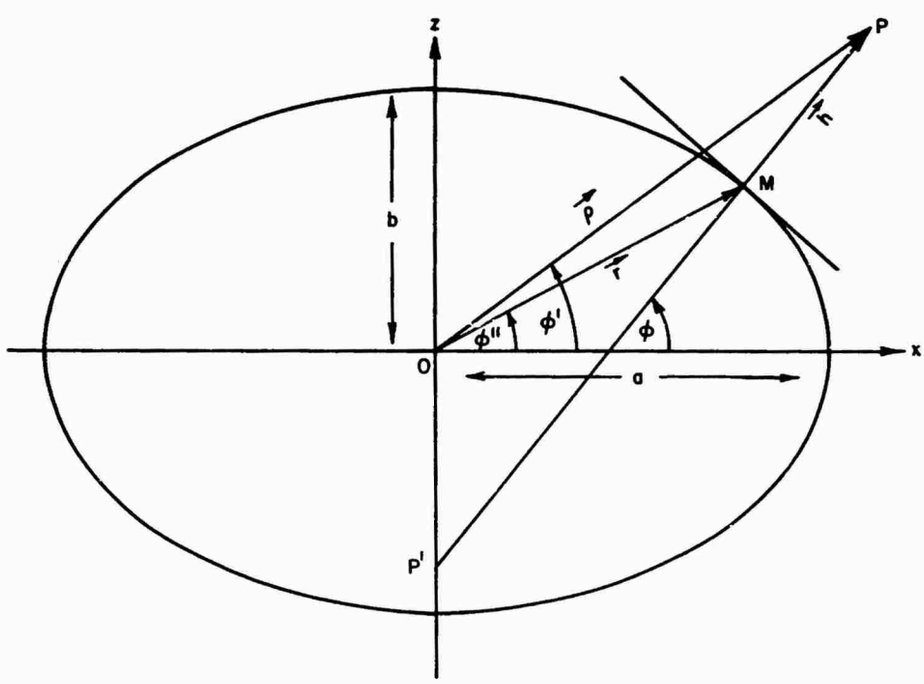

Figure 11. Geodetic System of Coordinates

7.2 Geodetic to Geocentric Coordinates

Transformations involving geodetic or horizon coordinates (azimuth and elevation) will now be discussed. From Figure 11 we can determine the geocentric coordinates of a point whose geodetic latitude, longitude, and elevation above the reference ellipsoid are ϕ, λ, and h, respectively. Let the geocentric coordinates be expressed in terms of the parameters, ϕ', λ', and ρ. Then, clearly,

$$\lambda' = \lambda \,. \tag{73}$$

From Figure 11 it follows that

$$\vec{r} = r\,(\hat{x}\cos\phi'' + \hat{z}\sin\phi'')\,, \tag{74}$$

$$\vec{h} = h\,(\hat{x}\cos\phi + \hat{z}\sin\phi)\,. \tag{75}$$

For the reference ellipsoid we can also write

$$\vec{r} = \hat{x}a\cos t + \hat{z}b\sin t\,, \tag{76}$$

where t is a parameter.

A unit vector tangent to the ellipsoid at M is given by

$$\hat{t} = \frac{-(a\sin t)\hat{x} + (b\cos t)\hat{z}}{\sqrt{a^2\sin^2 t + b^2\cos^2 t}}\,. \tag{77}$$

But

$$\vec{h}\cdot\hat{t} = 0 \qquad \text{(condition of perpendicularity)}\,.$$

Hence,

$$\tan t = (b/a)\tan\phi\,, \tag{78}$$

$$r = \sqrt{a^2\sin^2 t + b^2\cos^2 t}\,. \tag{79}$$

Since

$$\tan\phi'' = (b/a)\tan t = (b/a)^2 \tan\phi \tag{80}$$

and

$$(b/a)^2 = 1 - \epsilon^2 \quad (\epsilon = \text{eccentricity}) ,$$

it follows that

$$\vec{r} = a\left[\frac{\hat{x}\cos\phi + \hat{z}\,(1-\epsilon^2)\sin\phi}{\sqrt{1-\epsilon^2\sin^2\phi}}\right] . \tag{81}$$

The geocentric coordinates are found by rotating the vector $\vec{r}$ about the z axis to allow for the general longitudinal dependence of the data. The results are:

$$\vec{\rho} = \hat{x}\left[\frac{a}{\sqrt{1-\epsilon^2\sin^2\phi}} + h\right]\cos\phi\cos\lambda +$$

$$+ \hat{y}\left[\frac{a}{\sqrt{1-\epsilon^2\sin^2\phi}} + h\right]\cos\phi\sin\lambda +$$

$$+ \hat{z}\left[\frac{a(1-\epsilon^2)}{\sqrt{1-\epsilon^2\sin^2\phi}} + h\right]\sin\phi ; \tag{82}$$

$$\tan\phi' = \left[\frac{1-\epsilon^2 + (h/a)\sqrt{1-\epsilon^2\sin^2\phi}}{1 + (h/a)\sqrt{1-\epsilon^2\sin^2\phi}}\right]\tan\phi . \tag{83}$$

7.3 Geocentric to Geodetic Coordinates

The inverse transformation is best carried out by resorting to Lagrange's expansion. Let

$$\vec{\rho} = \rho\,(\hat{x}\cos\phi'\sin\lambda' + \hat{y}\cos\phi'\sin\lambda' + \hat{z}\sin\phi') , \tag{84}$$

$$\vec{h} = \vec{\rho} - \vec{r} = \rho\,(\hat{r}\cos\phi' + \hat{z}\sin\phi') , \tag{85}$$

where $\vec{r}$ is given by Eq. (76). From Eqs. (85), (76), and (77), and the condition of perpendicularity of $\vec{h}$ and $\hat{t}$ we have

$$\tan t = \frac{b\rho \sin\phi' + a^2\epsilon^2 \sin t}{a\,\rho \cos\phi'}$$

$$= (b/a)\tan\phi' + \frac{a}{\rho}\,\frac{\epsilon^2}{\cos\phi'}\,\sin t\,. \tag{86}$$

Since $\epsilon \ll 1$ and $\sin t = \tan t/(1 + \tan^2 t)^{1/2}$, the Lagrange expansion leads to the expression

$$\tan t = \sqrt{1-\epsilon^2}\left[\tan\phi' + \left(\frac{a}{\rho}\right)\epsilon^2 \frac{\tan\phi'}{\sqrt{1-\epsilon^2\sin^2\phi'}} + \right.$$

$$\left. + \frac{1}{2}\left(\frac{a}{\rho}\right)^2 \epsilon^4 \frac{\sin 2\phi'}{(1-\epsilon^2\sin^2\phi')^2}\right] + O(\epsilon^6)\,. \tag{87}$$

Once we know the value of the parameter t, we can immediately write

$$\vec{r} = a\,(\hat{r}\cos t + \hat{z}\sqrt{1-\epsilon^2}\,\sin t) \tag{88a}$$

and

$$\vec{h} = \hat{r}\,(\rho\cos\phi' - a\cos t) + \hat{z}\,(\rho\sin\phi' - a\sqrt{1-\epsilon^2}\sin t)\,. \tag{88b}$$

Hence,

$$h = \left[\rho^2 - 2a\rho\cos\phi'\cos t + \sqrt{1-\epsilon^2}\,\sin\phi'\,\sin t + a^2(1-\epsilon^2\sin^2 t)\right]^{1/2}, \tag{89}$$

$$\tan\phi = \frac{\rho\sin\phi' - a\sqrt{1-\epsilon^2}\,\sin t}{\rho\cos\phi' - a\cos t}\,, \tag{90}$$

$$\lambda = \lambda'\,. \tag{91}$$

7.4 Geocentric to Horizon Coordinates

The general transformation from geocentric to horizon coordinates involves a translation of the origin to the observation site, followed by rotations about the z and y axes, respectively. If the position vector in the horizon system is $\vec{\rho}_H$, it is such that

$$\vec{\rho}_H = \rho_H \begin{pmatrix} -\cos E \cos A \\ \cos E \sin A \\ \sin E \end{pmatrix},$$

where E is the elevation and A is the azimuth of the line of sight to the point being observed. Then

$$\rho_H \begin{pmatrix} -\cos E \cos A \\ \cos E \sin A \\ \sin E \end{pmatrix} = R_y\left(\frac{\pi}{2} - \phi'_s\right) R_z(\lambda_s) \left[\rho \begin{pmatrix} \cos\phi' \cos\lambda \\ \cos\phi' \sin\lambda \\ \sin\phi' \end{pmatrix} - r_s \begin{pmatrix} \cos\phi'_s \cos\lambda_s \\ \cos\phi'_s \sin\lambda_s \\ \sin\phi'_s \end{pmatrix}\right],$$

or,

$$\left(\frac{\rho_H}{\rho}\right) \begin{pmatrix} -\cos E \cos A \\ \cos E \sin A \\ \sin E \end{pmatrix} + \left(\frac{r_s}{\rho}\right) \begin{pmatrix} 0 \\ 0 \\ 1 \end{pmatrix} = \begin{pmatrix} \sin\phi'_s \cos\phi' \cos(\lambda - \lambda_s) - \cos\phi'_s \sin\phi' \\ \cos\phi' \sin(\lambda - \lambda_s) \\ \cos\phi'_s \cos\phi' \cos(\lambda - \lambda_s) + \sin\phi'_s \sin\phi' \end{pmatrix}, \quad (92)$$

where ϕ'_s and λ_s are the geocentric latitude and longitude of the observation site and r_s is the distance of the site from the geocentric origin. It can be verified that Eq. (92) leads to the relation

$$\left(\frac{\rho_H}{\rho}\right)^2 = 1 + \left(\frac{r_s}{\rho}\right)^2 - 2\left(\frac{r_s}{\rho}\right)\left[\cos\phi'_s \cos\phi' \cos(\lambda - \lambda_s) + \sin\phi'_s \sin\phi'\right].$$

The term in the brackets can be identified with the elevation of the line of sight to a target at a very great distance (a star, for example) and it is therefore convenient to set

$$\sin E_\infty = \cos\phi'_s \cos\phi' \cos(\lambda - \lambda_s) + \sin\phi'_s \sin\phi'. \quad (93)$$

Letting $m = r_s/\rho$ we can then write

$$\left(\frac{\rho_H}{\rho}\right)^2 = 1 + m^2 - 2m \sin E_\infty, \quad (94)$$

$$\sin E = \frac{-m + \sin E_\infty}{\sqrt{1 - 2m \sin E_\infty + m^2}}, \quad (95)$$

$$\tan A = \frac{\cos\phi' \sin(\lambda - \lambda_s)}{\cos\phi'_s \sin\phi' - \sin\phi'_s \cos\phi' \cos(\lambda - \lambda_s)} . \tag{96}$$

7.5 Horizon to Geocentric Coordinates (special case)

The transformation inverse to Eq. (92) is of importance only for very distant objects (stars). The transformation from horizon to geocentric coordinates in this special case is accomplished by application of the rotations $R_y^{-1}\left(\frac{\pi}{2} - \phi'_s\right)$ and $R_x^{-1}(\lambda_s)$ in succession. The results are

$$\sin\phi = \sin\phi'_s \sin E + \cos\phi'_s \cos E \cos A , \tag{97}$$

$$\tan\lambda = \frac{\sin E \sin\lambda_s \cos\phi' + \cos E(\cos\lambda_s \sin A - \sin\lambda_s \cos A \sin\phi'_s)}{\sin E \cos\lambda_s \cos\phi'_s - \cos E(\sin\lambda_s \sin A + \cos\lambda_s \cos A \sin\phi'_s)} . \tag{98}$$

7.6 Camera to Horizon Coordinates

The transformation from camera to horizon coordinates can be performed by combining a transformation from a camera to a geocentric system, followed by a transformation from a geocentric to a h zon system. Symbolically we can write

$$\begin{pmatrix} -\cos E \cos A \\ \cos E \sin A \\ \sin E \end{pmatrix} = R_y\left(\frac{\pi}{2} - \rho'_s\right) R_z\left(\lambda_s + \tau_G - \alpha_c\right) R_y^{-1}\left(\frac{\pi}{2} - \delta_c\right) R_z(-\delta\epsilon) \begin{pmatrix} \cos\eta \sin\sigma \\ \sin\eta \sin\sigma \\ \cos\sigma \end{pmatrix}, \tag{99a}$$

$$\rho = a_P , \tag{99b}$$

where a_P is the distance along the line of sight to the target being observed. It is determined from an expression of the form (59) or (69b).

If the orientation of the camera axis is referred to the geocentric system, the declination δ_c and right ascension α_c can be replaced by an effective latitude $\phi'_c = \delta_c$ and an effective longitude $\lambda_c = \alpha_c - \tau_G$. Equation (99a) then take the form

$$\begin{pmatrix} -\cos E \cos A \\ \cos E \sin A \\ \sin E \end{pmatrix} = R_y\left(\frac{\pi}{2} - \phi'_s\right) R_z(\lambda_s - \lambda_c) R_y^{-1}\left(\frac{\pi}{2} - \phi'_c\right) R_z(-\delta\epsilon) \begin{pmatrix} \cos\eta \sin\sigma \\ \sin\eta \cos\sigma \\ \cos\sigma \end{pmatrix} . \tag{100}$$

For the camera axis, $\sigma = 0$. Therefore, its azimuth and elevation are

$$\tan A_c = \frac{-\cos\phi'_c \sin(\lambda_s - \lambda_c)}{\cos\phi'_s \sin\phi'_c - \sin\phi'_s \cos\phi'_c \cos(\lambda_s - \lambda_c)} , \tag{101a}$$

$$\sin E_c = \sin\phi'_s \sin\phi'_c + \cos\phi'_s \cos\phi'_c \cos(\lambda_s - \lambda_c) . \tag{101b}$$

For hand computations it is convenient to write Eq. (100) in the form

$$\begin{pmatrix} -\cos E \cos A \\ \cos E \sin A \\ \sin E \end{pmatrix} = \begin{pmatrix} \sin\phi'_s \cos(\lambda_s - \lambda_c) & \sin\phi'_c \sin(\lambda_s - \lambda_c) & -\cos\phi'_s \\ -\sin(\lambda_s - \lambda_c) & \cos(\lambda_s - \lambda_c) & 0 \\ \cos\phi'_s \cos(\lambda_s - \lambda_c) & \cos\phi'_s \sin(\lambda_s - \lambda_c) & \sin\phi'_s \end{pmatrix} \begin{pmatrix} \cos\Omega \\ \sin\Omega \sin\Phi \\ \sin\Omega \cos\Phi \end{pmatrix} , \tag{102}$$

where

$$\cos\Omega = \cos\phi'_s \cos\sigma + \sin\phi'_c \sin\sigma \cos(\eta + \delta\epsilon) ,$$

$$\sin\Omega \cos\Phi = \sin\phi'_c \cos\sigma - \cos\phi'_c \sin\sigma \cos(\eta + \delta\epsilon) ,$$

$$\sin\Omega \sin\Phi = \sin\sigma \sin(\eta + \delta\epsilon) .$$

It can then be readily verified that

$$\sin E = \cos\sigma \sin E_c + \sin\sigma \cos E_c \cos(\eta + \delta\epsilon + \psi) , \tag{103}$$

$$\tan(A_c - A) = \frac{\sin(\eta + \delta\epsilon - \psi)}{\cos\sigma \cos E_c - \sin\sigma \sin E_c \cos(\eta + \delta\epsilon - \Psi)} , \tag{104}$$

where

$$\Psi = \tan^{-1}\left[\frac{-\cos\phi'_s \sin(\lambda_s - \lambda_c)}{\sin\phi'_s \cos\phi'_c - \cos\phi'_s \sin\phi'_c \cos(\lambda_s - \lambda_c)}\right] . \tag{105}$$

7.7 Horizon to Camera Coordinates

The transformation from horizon to camera coordinates is the inverse of the transformation given by Eq. (100), that is,

$$\begin{pmatrix} \cos\eta \sin\sigma \\ \sin\eta \sin\sigma \\ \cos\sigma \end{pmatrix} = R_z(\delta\epsilon) R_y\left(\frac{\pi}{2} - \phi'_c\right) R_z^{-1}(\lambda_s - \lambda_c) R_y^{-1}\left(\frac{\pi}{2} - \phi'_s\right) \begin{pmatrix} -\cos E \cos A \\ \cos E \sin A \\ \sin E \end{pmatrix}. \tag{106}$$

Since ordinarily the angular rotation of the film plane about the optic axis is known, it is convenient to premultiply both sides of Eq. (106) by $R_z^{-1}(\delta\epsilon)$ and write

$$\begin{pmatrix} \sin\sigma \cos(\eta + \delta\epsilon) \\ \sin\sigma \sin(\eta + \delta\epsilon) \\ \cos\sigma \end{pmatrix} = \begin{pmatrix} \sin\phi'_c & 0 & -\cos\phi'_c \\ 0 & 1 & 0 \\ \cos\phi'_c & 0 & \sin\phi'_c \end{pmatrix} \begin{pmatrix} \cos(\lambda_s - \lambda_c) & -\sin(\lambda_s - \lambda_c) & 0 \\ \sin(\lambda_s - \lambda_c) & \cos(\lambda_s - \lambda_c) & 0 \\ 0 & 0 & 1 \end{pmatrix} \times$$

$$\times \begin{pmatrix} \sin\phi'_s & 0 & \cos\phi'_s \\ 0 & 1 & 0 \\ -\cos\phi'_s & 0 & \sin\phi'_s \end{pmatrix} \begin{pmatrix} -\cos E \cos A \\ \cos E \sin A \\ \sin E \end{pmatrix}. \tag{107}$$

The zenith corresponds to a direction in space characterized by the camera coordinates η_z and σ_z obtained from Eq. (107) by setting $E = 90^\circ$. It follows, then, that

$$\cos\sigma_z = \sin\phi'_c \sin\phi'_s + \cos\phi'_c \cos\phi'_s \cos(\lambda_s - \lambda_c) = \sin E_c , \tag{108}$$

$$\tan(\eta_z + \delta\epsilon) = \frac{-\cos\phi'_s \sin(\lambda_s - \lambda_c)}{\sin\phi'_s \cos\phi'_c - \cos\phi'_s \sin\phi'_c \cos(\lambda_s - \lambda_c)} . \tag{109}$$

In Eq. (108) we have the analytic verification of the obvious relation $\sigma_z + E_c = 90^\circ$. For the general case we can write

$$\cos\sigma = \sin E \sin E_c + \cos E \cos E_c \cos(A - A_c) \tag{110}$$

and

$$\tan(\eta + \delta\epsilon - \Psi) = \frac{\cos E \sin(A_c - A)}{\sin E \cos E_c - \cos E \sin E_c \cos(A_c - A)} . \tag{111}$$

Comparison of Eqs. (105) and (109) shows that Eq. (111) can be written in the equivalent form

$$\tan(\eta_z - \eta) = \frac{\cos E \sin(A_c - A)}{\sin E \cos E_c - \cos E \sin E_c \cos(A_c - A)} . \tag{112}$$

Explicit expressions such as Eqs. (110) and (112) are useful when it is desired to do hand calculations. If computerized calculations are contemplated, it is more efficient and straightforward to use matrix relations such as Eq. (106). This is because we can have computer subroutines for the general rotations $R_y(\theta)$ and $R_z(\theta)$, and can generate the coordinate transformations by successive calls to the subroutines with appropriate values for the rotation angles.

References

Ahlberg, J.H., Nilson, E.N., and Walsh, J.L. (1967) The Theory of Splines and Their Applications, Academic Press.

Albritton, D.L., Young, L.C., Edwards, H.D., and Brown, J.L. (1962), in Photogrammetric Engineering, September 1962, pp. 608-614.

Bekey, G.A. and McGhee, R.B. (1964) Gradient methods for the optimization of dynamic system parameters by hybrid computation, in Conf. on Computing Methods in Optimization Problems (Los Angeles, 1964), Academic Press.

Bellman, R. (1964) Perturbation Techniques in Mathematics, Physics, and Engineering, Holt, Rinehart and Winston.

Boehmer, R.P. (1970) A Three-Station Method to Acquire Smoke Trail Position, Final Report, Dayton U. Res. Inst., AFCRL-70-262(AD-709895).

Edwards, H.D. (1963) Photographic and Photometric Observations of Chemical Releases, Data Reduction, Interpretation and Analysis, Interim Tech. Rpt, Georgia Inst. Tech., Contracts AF19(628)-393 and AF19(628)-3305.

Justus, C.G. (1963) A Method Employing Star Backgrounds for Improving the Accuracy of the Location of Clouds or Objects in Space from Data Recorded on Film, MS Thesis, Georgia Inst. Tech.

Justus, C.G., Edwards, H.D., and Fuller, R.N. (1964) Analysis Techniques for Determining Mass Motions in the Upper Atmosphere From Chemical Releases, Sci. Rpt No. 1, Georgia Inst. Tech., Contract AF19(628)-3305.

Kaula, W.M. (1966) Theory of Satellite Geodesy, Blaisdell, Waltham, Mass.

Mueller, I.I. (1969) Spherical and Practical Astronomy as Applied to Geodesy, Frederick Ungar Publishing Co., New York

Smirnov, V.I. (1961) Linear Algebra and Group Theory, McGraw-Hill.

Uvarov, D.B. (1969) Determination of the Positions of Artificial Noctilucent Clouds or Positions of Meteor Trains by Transformation of Coordinates, translated from Astronomicheskii Vestnik 3(No. 1):50-56.

Preceding page blank

Preceding page blank

Appendix A

Parametric Cubic Splines

In the ordinary treatment of cubic splines (Ahlberg, Nilson, and Walsh), we consider an interval $a \leq x \leq b$ and subdivide it by a mesh of points corresponding to the locations of the data points:

$$a = x_1 < x_2 < \cdots < x_{N+1} = b.$$

The associated set of ordinates is

$$y_1, y_2, y_3, \ldots, y_{N+1} .$$

We denote the set of mesh points by Δ and the set of ordinates by Y. We then seek a function $S_\Delta(Y, x)$ that is continuous together with its first and second derivatives in the interval (a, b) and is represented in each subinterval by a cubic polynomial in x. If we write the ith polynomial in the form

$$y - y_i = a_i(x - x_i) + b_i(x - x_i)^2 + c_i(x - x_i)^3 , \quad i = 1, 2, 3, \ldots, N , \tag{A1}$$

the spline function is defined when all the coefficients a_i, b_i, c_i are known. Since there are N intervals, the total number of unknown coefficients is 3N. To determine these coefficients we have 3(N-1) continuity conditions at N-1 internal mesh points. A further condition arises from the Nth polynomial, which, evaluated at $x = x_{N+1}$, must lead to $y = y_{N+1}$.

A unique solution requires the introduction of two additional conditions. One of the simplest ways of accomplishing this is to take

$$S_{\Delta}^{(p)}(a+) = S_{\Delta}^{(p)}(b-), \quad p = 0, 1, 2 .$$

The spline is then said to be periodic, of period (b-a). For nonperiodic splines the two conditions may consist in specifying the end slopes or requiring that the curvature at the ends be zero. It can be shown that the periodic cubic spline with prescribed ordinates at mesh points always exists and is unique. The same is true of nonperiodic splines having the end slopes prescribed, of splines having prescribed second derivatives at the ends, or those satisfying the conditions $S''_{\Delta}(a) = \lambda S''_{\Delta}(x_2)$; $S''_{\Delta}(x_{N+1}) = \mu\, S''_{\Delta}(x_N)$, when both λ and μ are numbers between 0 and 1.

Spline functions composed of polynomials of type (A1) are adequate for approximating single-valued functions of x. Multivalued functions can be handled if a parametric representation is introduced. The most suitable parameter is the cumulative chordal distance that at point $P_j(x_j, y_j)$ is

$$s_j = \sum_{i=2}^{j} \left[(x_i - x_{i-1})^2 + (y_i - y_{i-1})^2\right]^{1/2}, \quad j = 2, 3, 4, \ldots, N+1 . \tag{A2}$$

The problem is to spline-fit x and y as functions of the parameter s. Note that the inclusion of multivalued functions requires us to compute two sets of 3N polynomial coefficients.

Let us denote the spline functions for x and y by $S_{\Delta}(X, s)$ and $S_{\Delta}(Y, s)$, respectively. The mesh Δ corresponds to the set of s values

$$0 = s_1 < s_2 < s_3 < \ldots < s_{N+1} .$$

The cubic polynomials for the ith subinterval are then

$$x - x_i = a_i^{(x)}(s-s_i) + b_i^{(x)}(s-s_i)^2 + c_i^{(x)}(s-s_i)^3 , \tag{A3}$$

$$y - y_i = a_i^{(y)}(s-s_i) + b_i^{(y)}(s-s_i)^2 + c_i^{(y)}(s-s_i)^3 . \tag{A4}$$

Because of the relations

$$\frac{dy}{dx} = \frac{\dot{y}}{\dot{x}} ,$$

$$\frac{dy^2}{dx^2} = \frac{\dot{x}\,\ddot{y} - \dot{y}\,\ddot{x}}{(\dot{x})^3} ,$$

where the dot represents differentiation with respect to s, the conditions for matching slopes and second derivatives for the function $y = y(x)$ at the interval mesh points $P_i(x_i, y_i)$ are translated into corresponding matches of the slopes and second derivatives for each of the spline functions $S_\Delta(X, s)$ and $S_\Delta(Y, s)$.

If the curvature at the ends is to vanish, the following conditions have to be satisfied:

At s_1, $\ddot{x} = \ddot{y} = 0$. Consequently,

$$b_1^{(x)} = b_1^{(y)} = 0 .$$

At s_{N+1}, $\ddot{x} = \ddot{y} = 0$. Hence,

$$b_N^{(x)} + 3c_N^{(x)}(s_{N+1} - s_N) = 0 ,$$

$$b_N^{(y)} + 3c_N^{(y)}(s_{N+1} - s_N) = 0 .$$

The coefficients for the x and y splines are determined by repeated application of the following basic procedure.

Let $d_i = s_{i+1} - s_i$ and let ξ_i be either $(x_{i+1} - x_i)/d_i$ or $(y_{i+1} - y_1)/d_i$. At internal points we have:

$$\xi_i = a_i + d_i b_i + c_i d_i^2 , \quad i = 1, 2, \ldots, N , \tag{A5}$$

$$a_{i+1} = a_i + 2b_i d_i + 3\, c_i d_i^2 , \quad i = 1, 2, \ldots, N-1 , \tag{A6}$$

$$b_{i+1} = b_i + 3c_i d_i , \quad i = 1, 2, \ldots, N-1 . \tag{A7}$$

From these equations it follows that

$$d_i b_i = 3\xi_i - a_{i+1} - 2a_i ,$$

$$3c_i d_i^2 = 3\left(\xi_{i+1}\frac{d_i}{d_{i+1}} - \xi_i\right) - \frac{d_i}{d_{i+1}}a_{i+2} - a_{i+1}\left(\frac{2d_i}{d_{i+1}} - 1\right) + 2a_i,$$

and therefore

$$\left(\frac{d_{i+1}}{d_i + d_{i+1}}\right)a_i + 2a_{i+1} + \left(\frac{d_i}{d_i + d_{i+1}}\right)a_{i+2}$$

$$= 3\left(\frac{d_{i+1}}{d_i + d_{i+1}}\right)\xi_i + 3\left(\frac{d_i}{d_i + d_{i+1}}\right)\xi_{i+1}, \quad i = 1, 2, 3, \ldots, N-1.$$

Furthermore, the zero curvatore conditions lead to the relations

$$2a_1 + a_2 = 3\xi_1,$$

$$a_N + 2a_{N+1} = 3\xi_N.$$

Let

$$\lambda_i = \frac{1}{1 + (d_i/d_{i+1})}, \quad \mu_i = 1 - \lambda_i.$$

Then the equations to determine the <u>a</u> coefficients can be written in the form

$$\begin{aligned}
2a_1 + a_2 &= 3\xi_1, \\
\lambda_1 a_1 + 2a_2 + \mu_1 a_3 &= 3(\lambda_1\xi_1 + \mu_1\xi_2), \\
\lambda_2 a_2 + 2a_3 + \mu_2 a_4 &= 3(\lambda_2\xi_2 + \mu_2\xi_3), \\
&\ldots \\
\lambda_i a_i + 2a_{i+1} + \mu_i a_{i+2} &= 3(\lambda_i\xi_i + \mu_i\xi_{i+1}), \\
&\ldots \\
\lambda_{N-1}a_{N-1} + 2a_N + \mu_{N-1}a_{N+1} &= 3(\lambda_{N-1}\xi_{N-1} + \mu_{N-1}\xi_N), \\
a_N + 2a_{N+1} &= 3\xi_N.
\end{aligned}$$

This tridiagonal system has been discussed in detail in the literature (Smirnov, 1961). The recurrence relations that are obtained are well adapted to digital computer implementation.

Figure A1 shows the results of a parametric fit to the synthetic data listed in the upper right corner of the figure.

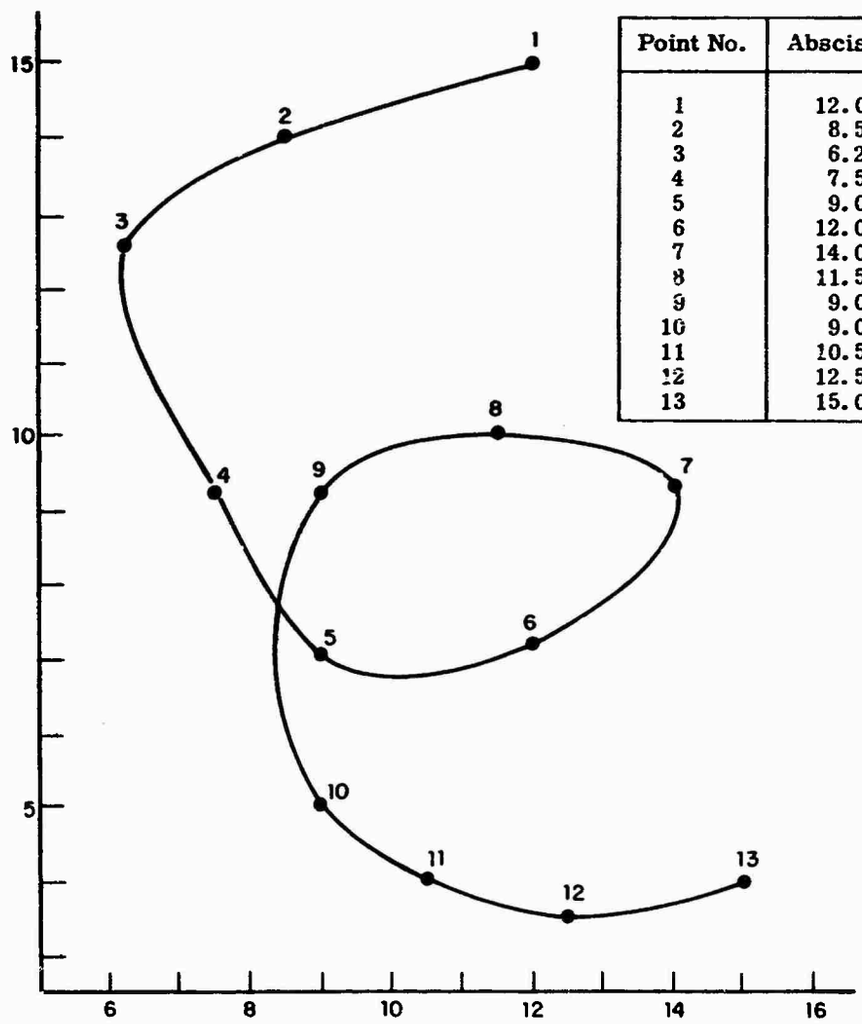

Point No.	Abscissa	Ordinate
1	12.0	15.0
2	8.5	14.0
3	6.2	12.5
4	7.5	9.2
5	9.0	7.0
6	12.0	7.2
7	14.0	9.2
8	11.5	10.0
9	9.0	9.2
10	9.0	5.0
11	10.5	4.0
12	12.5	3.5
13	15.0	4.0

Figure A1. Example of Curve-fitting by Means of Parametric Cubic Splines

Preceding page blank

Appendix B

Lagrange's Expansion

Let f(z) and g(z) be functions of z, analytic on and inside a contour C that surrounds the point $z = \alpha$. Let ϵ be such that the following inequality is satisfied for all points on the perimeter of C:

$$|\epsilon g(z)| < |z-\alpha| .$$

Then

$$u = \alpha + \epsilon g(u)$$

has precisely one root* in the interior of C, $u = u(\alpha)$; and f(u), which is analytic on and inside C, can be written in the form

$$f(u) = f(\alpha) + \sum_{1}^{\infty} \frac{\epsilon^n}{n!} \left(\frac{d}{d\alpha}\right)^{n-1} \left\{ f'(\alpha) [g(\alpha)]^n \right\} . \tag{B1}$$

This is the Lagrange expansion (Bellman, 1964).

* This is a consequence of the following lemma: Let f(z) and $\phi(z)$ be analytic in the interior of a closed curve C, continuous on the curve itself and such that on the entire curve $|\phi(z)| < |f(z)|$. Then the two equations f(z) = 0 and $f(z) + \phi(z) = 0$ have the same number of roots in the interior of C.

Let us apply this result to Eq. (86)

$$\tan t = \left(\frac{b}{a}\right) \tan\phi' + \frac{a}{\rho} \frac{\epsilon_o^2}{\cos\phi'} \sin t ,$$

with ϵ changed to ϵ_o to avoid confusion with the ϵ that appears in Eq. (B1).

We introduce the following identification:

$$u = \tan t$$

$$\alpha = \left(\frac{b}{a}\right) \tan\phi'$$

$$g(u) = \left(\frac{a}{\rho}\right)\frac{\sin t}{\cos\phi'} = \left(\frac{a}{\rho}\right) \frac{\tan t}{\cos\phi'\sqrt{1 + \tan^2 t}} = \left(\frac{a}{\rho}\right) \frac{u}{\cos\phi'\sqrt{1 + u^2}}$$

$$\epsilon = \epsilon_o^2$$

$$f(u) = u, \quad f'(u) = 1 .$$

According to Eq. (B1) we can then write:

$$u = \alpha + \sum_1^\infty \frac{\epsilon^n}{n!} \left(\frac{d}{d\alpha}\right)^{n-1} \left(\frac{a\alpha}{\rho \cos\phi' \sqrt{1 + \alpha^2}}\right)^n$$

$$= \alpha + \frac{\epsilon}{1} \left(\frac{a\alpha}{\rho \cos\phi' \sqrt{1 + \alpha^2}}\right) + \frac{\epsilon^2}{2!} \left(\frac{a}{\rho \cos\phi'}\right)^2 \left(\frac{2\alpha}{(1 + \alpha^2)^2}\right) + O(\epsilon^4) ,$$

that is,

$$\tan t = \left(\frac{b}{a}\right) \tan\phi' + \epsilon_o^2 \left(\frac{a}{\rho}\right)\left(\frac{b}{a}\right) \frac{\tan\phi'}{\sqrt{\left(1 - \epsilon_o^2 \sin^2\phi'\right)}} +$$

$$+ \frac{1}{2} \epsilon_o^4 \left(\frac{a}{\rho}\right)^2 \left(\frac{b}{a}\right) \frac{\sin 2\phi'}{\left(1 - \epsilon_o^2 \sin^2\phi'\right)^2} + O(\epsilon_o^6) .$$

Substitution of $\frac{b}{a} \sqrt{1 - \epsilon_o^2}$ leads to Eq. (87) .

Appendix C

Useful Constants

Time Constants

Period of rotation of earth: $23^h56^m04.1^s$ mean solar time

One uniform sidereal day: $23^h56^m04.091^s$ mean solar time

One mean solar day: $24^h03^m56.555^s$ uniform sidereal time

Tropical Year: 366.2422 mean sidereal days
365.2424 mean solar days

Sidereal Year: 366.2564 mean sidereal days
365.2504 mean solar days

Astrodynamic Constants

Rotational rate $(\omega) = 0.729211514\ (6) \times 10^{-4}$ rad/sec

Mass of earth $(M) = 5.975(1 \pm 0.0007) \times 10^{27}$ gm

Constants for Geographic Ellipsoids

Author, Date	a_e(m)	1/f	Countries using ellipsoid
Clarke, 1866	6,378,206	294.98	United States, Canada, Mexico
Clarke, 1880	6,378,249	293.47	France, South Africa
Everest, 1830	6,377,253	300.80	India
Plessis	6,376,523	308.64	France (mapping)
Bessel, 1841	6,377,397	299.15	Germany, Austria, Dutch East Indies
Kraijenhoff	6,376,950	309.65	Holland
Danish survey	6,377,019	300	Denmark

Constants for International Ellipsoid

Semimajor axis (equatorial radius) = 6,378,388 m

Flattening = 1/297 = 0.003 367 003 4

Polar radius = 6,356,911.946 m

Square of eccentricity = 0.006 722 670

Length of quadrant of the equator = 10,019,148.4 m

Length of quadrant of the meridian = 10,002,288.3 m

Area of the ellipsoid = 510,100,934 sq km

Volume of the ellipsoid = 1,083,319,780,000 cu km

Radius of sphere having same area as ellipsoid = 6,371,227.7 m

Radius of sphere having same volume as ellipsoid = 6,371,221.3 m

Mass of the ellipsoid = 5.998×10^{21} metric tons

Mean density = 5.527